

Collection system optimization for hybrid power plants



Department of
Wind Energy
Master Report

Claudia Maria Roselló Abad

DTU Wind Energy-M-0480

July 2021

Author: Claudia Maria Roselló Abad

Title: Collection system optimization for hybrid power plants

DTU Wind Energy-M-0480

July 2021

Project period:

February – July 2021

ECTS: 30

Education: Master of Science

Supervisors:

Katherine Dykes

Kaushik Das

Nicolaos Antonio Cutululis

Juan-Andrés Pérez-Rúa

DTU Wind Energy

Remarks:

This report is submitted as partial fulfillment of the requirements for graduation in the above education at the Technical University of Denmark.

DTU Wind Energy is a department of the Technical University of Denmark with a unique integration of research, education, innovation and public/private sector consulting in the field of wind energy. Our activities develop new opportunities and technology for the global and Danish exploitation of wind energy. Research focuses on key technical-scientific fields, which are central for the development, innovation and use of wind energy and provides the basis for advanced education at the education.

Technical University of Denmark

Department of Wind Energy

Frederiksborgvej 399

4000 Roskilde

Denmark

www.vindenergi.dtu.dk

Abstract

Long has it been voiced by experts from the energy industry that the major challenge for the expansive deployment of renewable energies is their intrinsic intermittency. The concept of Hybrid Power Plants (HPPs) emerges as a promising alternative as it allows smoothing of fluctuations due to the complementary effects of the technologies. So far, studies have mainly focused on sizing and operation of HPPs. There is thus a further need to investigate the electrical infrastructure and notably its optimization through the use of mathematical models.

In that setting, the present project addresses the design of the optimal electrical collection system of a HPP which integrates onshore wind and solar photovoltaic (PV), in order to save costs while increasing the electrical infrastructure utilization. For this purpose, an optimization model is built and solved using the Branch-and-Cut solver implemented in IBM ILOG CPLEX, in Python.

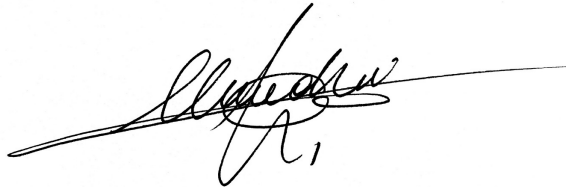
By means of this thesis it is proven that designing a shared electrical infrastructure for the two generation technologies leads to significant savings both in terms of investment cables cost and cost associated to curtailed energy. The extracted results reveal that the implementation of the proposed solution, increases the economic profitability by 20.26%. Moreover, unlike what has been carried out up to the present for the cables dimensioning, consisting of assuming nominal power operation of the generators throughout the HPP's lifetime, the use of more realistic power values that reflect the negative correlation of the renewable energy sources (RES) leads to an increase of economic profitability of 39.46%.

Overall, it is foreseen the present study to be of crucial interest for broader and more inclusive models targeting the design of the collection system of HPPs, due to the aforementioned higher profitability. The application of the model to real-life problems is expected to have a significant impact, thus triggering the deployment of HPPs.

Preface

This Master thesis was prepared at the department of Wind Energy at the Technical University of Denmark in fulfillment of the requirements for acquiring a Master degree in Sustainable Energy.

Copenhagen, July 16, 2021

A handwritten signature in black ink, appearing to read 'Claudia Roselló', with a long horizontal line extending to the right and a small '1' written below the signature.

Claudia María Roselló Abad (s192491)

Acknowledgements

First and foremost I would like to express my sincere gratitude to my supervisor Juan-Andrés Pérez Rúa, for his invaluable help, involvement and guidance throughout the entire project. I would also like to thank my supervisors Katherine Dykes and Kaushik Das for providing support and useful suggestions and for giving me the opportunity to develop this project. I must also thank Carlos Roldán Blay, my supervisor at UPV for his support and for being a big inspiration all these years.

I want to deeply thank my friends, especially David, Marina, Madeleine, Laura and Albert, for being my pillars and the greatest sources of joy during this journey. For standing by my side, motivating and supporting me all this time.

Thanks to DTU and my home university UPV for allowing me to grow personally and professionally and get to where I am now.

Finally, I wish to show my appreciation to my family, my Mom, my Dad, Blanca, Carlos and Miguel, who have always been there for me, and for their unconditional love and encouragement.

Contents

Abstract	i
Preface	iii
Acknowledgements	v
Contents	vii
List of Figures	ix
List of Tables	xi
Abbreviations	xiii
1 Introduction	1
1.1 Motivation	1
1.2 Problem definition, assumptions and limitations	4
2 Literature Review	7
2.1 Background on Hybrid Power Plants	7
2.2 Advantages and Functionalities	10
2.3 Market Opportunities	12
2.4 Power electronics topologies	13
2.5 Large scale photovoltaic power plants	14
2.6 Large scale wind farms	19
3 Definition of model inputs	23
3.1 Generation technologies specifications	24
3.2 HPP configuration design	25
3.3 Energy conversion and transmission equipment specifications	34
3.4 Data collection	36
4 Collection System Design	41
4.1 Problem description	41
4.2 Graph and model representation	43

4.3	MILP Model	46
5	Results and Discussion	49
5.1	Test 1	49
5.2	Test 2	53
5.3	Test 3	53
6	Conclusions and Future work	63
6.1	Conclusions	63
6.2	Recommendations for Future work	64
	Bibliography	65
	Appendix	69
	Test 2 - Additional plots	69
	Test 3 - Additional plots	72

List of Figures

List of Figures	x
1.1 Global power investment by generation source [4].	2
1.2 Impact on levelised cost of electricity for newly commissioned renewable power capacity [4].	2
1.3 HPP collection system design and optimization: Decision flowchart. . .	5
2.1 Types of HPPS in terms of integration and operation of different generating modules.[11]	9
2.2 Configurations for: I. Co-Located HPP. II. WTG-coupled system integration. III. DC-coupled HPP for HVAC connection. IV. DC-coupled HPP for HVDC connection [12].	10
2.3 Foreseen benefits of wind-solar HPPs [11].	11
2.4 Grid-connected hybrid system [13]	14
2.5 Comparison of market available PV inverter topologies for LS-PVPPs [14].	16
2.6 Connection of transformers at medium voltage. (a) Central PV inverter with three winding transformer and (b) multistring PV inverter with two winding transformer [14].	17
2.7 PV inverter topologies. (a) Central, (b) string, (c) multistring, and (d) module integrated [14].	19
3.1 Inputs for the Optimization problem.	23
3.2 Internal PV system setup.	27
3.3 HPP layout 2 including 20 WTs and 3 PV systems.	29
3.4 HPP layout 3 including 20 WTs and 8 PV systems.	29
3.5 Procedure for establishing the set of Tests to be evaluated for the optimization.	30
3.6 Configuration with individual step-up transformer per energy source. .	31
3.7 Configuration with shared step-up transformer for both energy sources.	32
3.8 One year solar and wind time series normalized for 20 WTs and 1 PV system.	37

3.9	One year solar and wind time series normalized for 20 WTs and 3 PV systems.	37
3.10	One year solar and wind time series normalized for 20 WTs and 8 PV systems.	37
3.11	Cables cost coefficients.	39
4.1	Collection system Optimization process: flow diagram.	43
5.1	Optimal collection system layout when applying strategy 0 to Test 1.	51
5.2	Optimal collection system layout when applying strategy 1 to Test 1.	51
5.3	Optimal collection system layout when applying strategy 2 to Test 1.	52
5.4	Optimal collection system layout when applying strategy 3 to Test 1.	52
5.5	Optimal collection system layout when applying strategy 0 to Test 3.	55
5.6	Optimal collection system layout when applying strategy 1 to Test 3.	55
5.7	Optimal collection system layout for the base case of Test 3.	56
5.8	Optimal collection system layout for the base case of Test 3 layout when forcing PV systems to be connected in series.	57
5.9	Top: Time-series of power generated by 8 WTs over 1 week. Middle: Time-series of power generated by 3 PV systems over 1 week. Bottom: Power flow through cable 0-8 connecting 8 WTs and 3 PV systems over 1 week (3600 hour to 3800 hours.	59
5.10	Optimal collection system layout when applying strategy 1 to Test 3 with an electricity price of 100€/MWh.	60
5.11	Optimal collection system layout when testing an electricity price of 100€/MWh in the Base Case.	61
1	Optimal collection system layout when applying strategy 0 to Test 2.	69
2	Optimal collection system layout when applying strategy 1 to Test 2.	70
3	Optimal collection system layout when applying strategy 2 to Test 2.	70
4	Optimal collection system layout when applying strategy 3 to Test 2.	71
5	Optimal collection system layout when applying strategy 2 to Test 3.	72
6	Optimal collection system layout when applying strategy 3 to Test 3.	73

List of Tables

List of Tables	xi
3.1 Technical characteristics of installed wind turbines.	24
3.2 Technical characteristics of installed PV modules.	25
3.3 Considerations for design of WTs layout.	26
3.4 Internal PV system considerations.	26
3.5 Basic information on the real-world cables used for the HPP collection system.	34
3.6 Capacities of cables used in the project.	35
5.1 Optimal solution results for Test 1.	50
5.2 Optimal solution results for Test 2.	53
5.3 Optimal solution results for Test 3.	54
5.4 Overview of results obtained from the evaluation of Test 6.	58

Abbreviations

AC	Alternating Current
a-Si	Amorphous Silicon
BoP	Balance-of Plant
BOS	Balance of System
CdTe	Cadmium Telluride
CIGS/CIS	Copper Indium (Gallium) Di-Selenide
c-Si	Crystalline silicon
DC	Direct Current
GHG	Greenhouse Gas
HPP	Hybrid Power Plant
HRES	Hybrid Renewable Energy Source
HV	High Voltage
kA	Kiloampere
kV	Kilovolt
kWh	Kilo Watt Hour
LCOE	Levelized Cost of Energy
LS-PVPP	Large Scale Photovoltaic Power Plant
MILP	Mixed Integer Linear Programming
mono-c-Si	Mono-Crystalline silicon
MPPT	Maximum Power Point Tracking
multi-c-Si	Multi-Crystalline silicon
MW	Mega Watt

MWh	Mega Watt Hour
M€	Million euro
NPV	Net Present Value
PCC	Point of Common Coupling
PID	Potential Induced Degradation
PV	Photovoltaic
RES	Renewable Energy Source
TWh	Tera Watt Hour
USD	American Dollar
W	Watt
WT(s)	Wind Turbine(s)
5D	5 diameters
8D	8 diameters

CHAPTER 1

Introduction

1.1 Motivation

For many years, fossil fuels have had a dominant deployment compared to renewable energy technologies in electric power systems. Nevertheless, this tendency has changed considerably in recent times since renewables have gained maturity and innovative solutions and technologies start delivering on the promise of a clean energy future. This, in turn, has led to a reduction of wind and solar costs, making them economically competitive against conventional power plants. As a matter of fact, studies forecast that the fast ramping up of renewables will make the share of solar photovoltaic (PV) and wind in the electricity mix reach a value of 31% by 2050, displacing fossil fuels and diminishing considerably their contribution to 17% [1]. In addition, the growing environmental concern and awareness of governments and the population, together with global treaties and policies ([2], [3]), have driven renewable energies to be the ever-increasing dominant choice for new electricity generation systems. Of all renewable energy technologies, solar and wind have proved to be the most competitive. For that reason, as illustrated in Figure 1.1, they are the technologies in which it has been invested the most [4]. Even if significant cost reductions in wind and solar PV have been reached (Figure 1.2), these technologies are not free of inherent drawbacks. Variability, uncertainty, low dispatchability, unavailability, unpredictability and low electric grid reliability, are some of them. [5].

As a result, a discussion is currently open about the possibility of combining different renewable sources, e.g., wind, solar photovoltaic, and potentially a storage technology, to mitigate some of the problems mentioned above and to compensate for the weaknesses of one with the strengths of another. This proposed solution is known as Hybrid Power Plant (HPP) and there is a wide range of arguments that supports its development. Some projects have even been recently deployed, being the most famous the Kennedy Park in Australia, fruit of a joint collaboration between Vestas and Winlab [6].

The present study focuses on hybrid power plants consisting of wind and solar. When combining the latter technologies as a single power plant, it is shown that numerous advantages can be attained, with respect to their independent

development. This may obey to the negative correlation they exhibit. Indeed, this raises an intriguing question regarding the feasibility and cost-effectiveness of proposing a shared electrical infrastructure for the two generation technologies, rather than designing independent cable routings. The aim is to exploit the potential derived from the geographical proximity and negative correlation of the generation sources.

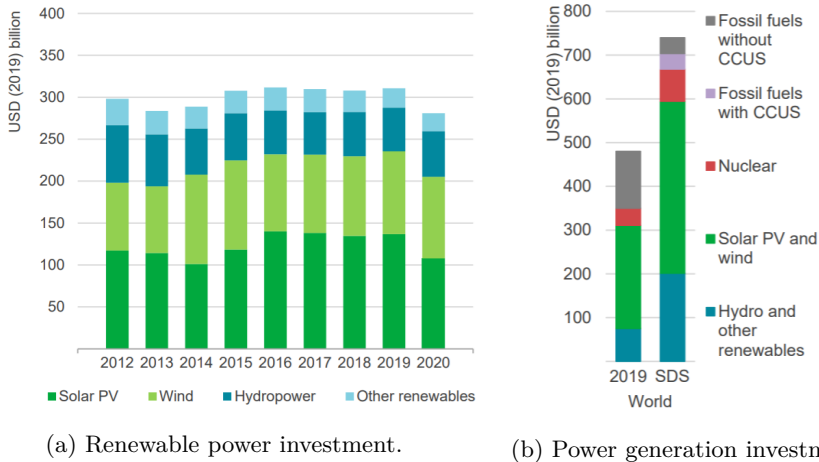


Figure 1.1: Global power investment by generation source [4].

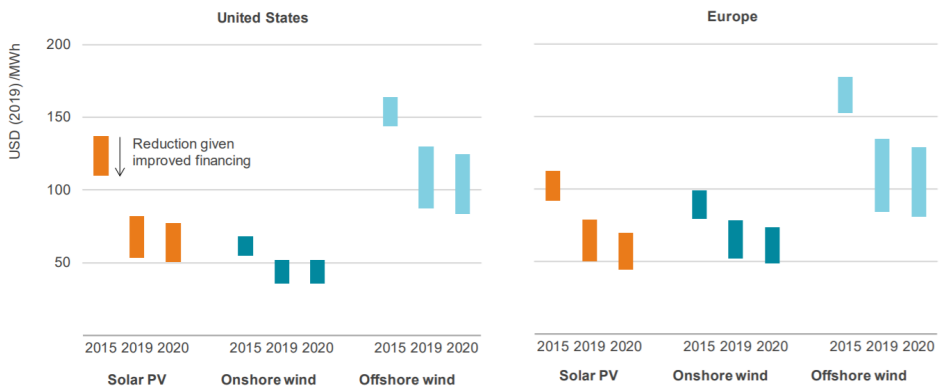


Figure 1.2: Impact on levelised cost of electricity for newly commissioned renewable power capacity [4].

Regarding the participation in energy markets, renewable energy sources (RES) have encountered in general more hurdles to take part on them, as compared to fossil fuels which have a stronger presence [5]. This is mainly a consequence of their intrinsic variability and unpredictability. In that setting, HPPs can be game-changers to ensure, in the coming future, a key place for renewables in energy markets and an ever more substantial share in the energy mix. The reason behind the success of this energy generation alternative is its resemblance to conventional power plants in terms of operation. Thus, allowing to provide ancillary and other services to support the stability of the grid, as well as presenting a higher dispatchability and reliability in a market characterized by time-varying energy prices. This supposes a meaningful shift from old classic procedures as the new operation mode consists of consistently producing power below the rated capacity, over dimensioning each technology and providing energy when demanded.

This subject opens up a new field of investigation that involves numerous subtopics: analysis and selection of technologies to be combined, sizing of the plant, decision on the overall topology, design of physical considerations, research of innovation opportunities, and optimization of plant operation and control. Notably, the coupling of the hybrid plant with the electrical system is of significant importance and is considered as one of the most relevant subjects of study for ongoing research. Hence, this Master Thesis focuses on the design and optimization of the electrical infrastructure of HPPs and the combination and integration of Balance-of Plant (BoP) elements. It intends to provide an answer to the question formulated above concerning the possibility of sharing electrical infrastructure, leaving aside the traditional procedure carried up to the present.

The challenge of designing the cable routing network of the plant is of notable interest because its cost, including both the cables and other electrical equipment, presents the second most significant share in HPP budgets [7]. Consequently, finding the optimal electrical network in terms of investment costs and curtailed energy may provide great potential through performance of computational optimization.

Nevertheless, since the current number of HPP projects under development or in operation is limited, and the topic is fairly new, there is little literature on the subject. This hinders access to existing specific data about the collection system design of an HPP, which leads to several assumptions throughout the project.

1.2 Problem definition, assumptions and limitations

An optimisation program is proposed in this thesis where two generation technologies, namely wind and solar PV are integrated, presenting common cable routing (also referred to as cable layout, collection layout or collection system). Additionally, the concept of overplanting is deployed since the installed wind and solar powers are higher than the grid rated capacity. Regarding the coupling between the HPP and the grid, this is carried out through a unique substation and unique connection point, referred to as Point of Common Coupling (PCC), from this point forward. Two main drivers make this an attractive research subject. They are as follows: the geographical proximity of PV modules with respect to the WTs and the PCC, and the complementarity of wind and solar energy resources. For the above-mentioned reasons, the purpose of installing independent collection networks for each technology is questioned, as it leads to potential under usage of cables, contrarily to what occurs when sharing electrical infrastructure, that instead results in an utilisation factor increase.

The optimisation aims to find the collection network that results in lowest investment costs while minimising curtailment, due to operation of the HPP throughout its lifetime. A mathematical optimisation model is built encompassing three types of decision variables: investment (the design of the electrical system per se), flow through the electrical system and curtailment in the generation units. Several constraints related to, e.g., power flow capacities through cables, curtailment in generation nodes, grid rated capacity and flow conservation are considered. The goal of the project is to develop an optimisation tool that allows providing the best electrical layout for a number of study cases where different parameters are modified, i.e., number of WTs and PV systems installed, electricity price, grid rated power and available cables. The extracted results are then compared to determine which strategy provides a better NPV value. These strategies consist of the clustering techniques applied to the power time-series data, used to reduce the problem's complexity (see Section 3.4.1). As it can be seen in Figure 1.3, the selection of the clustering strategy directly affects the collection system design and thus, the investment, flow and curtailment variables, as well as the optimal solution value. Subsequently, the trade-offs between the degree of realism of the clustering strategy and the best obtained solution can be assessed.

A flow diagram of the procedure conducted to develop the present project is illustrated in Figure 1.3. It entails, in the first place, the determination of the installed capacities of wind and solar PV, along with the number of turbines and modules needed. Also, the establishment of the grid rated capacity, performed by implementing the overplanting concept (further elaborated in Section 3.2.2).

This is followed by the integration and location of both technologies on the same site, by taking into consideration technical constraints, e.g., spacing, voltage level, and connection to inverters and transformers. Finally, the generated inputs, i.e., cables cost, electricity price and power time series, are introduced in the optimization problem to calculate the optimal cable layout and its corresponding solution value.

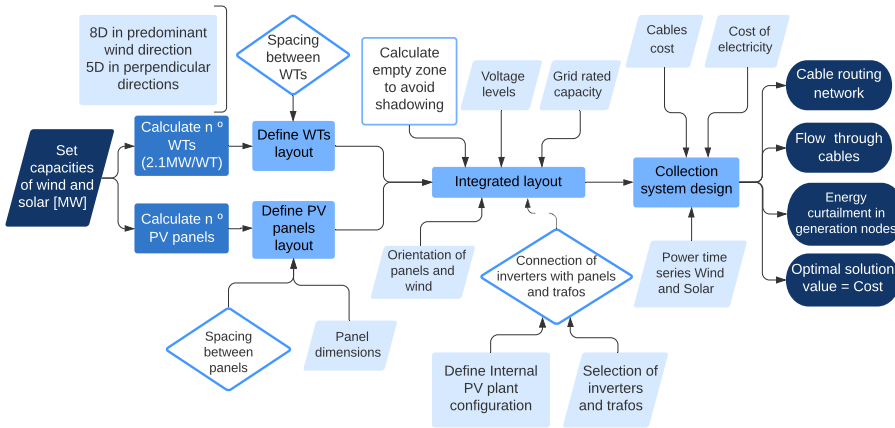


Figure 1.3: HPP collection system design and optimization: Decision flowchart.

The limitations and main sources of uncertainty identified throughout the study are identified, being mainly related to data collection, model choice and constraint definition. On that basis, certain assumptions are made during the development of the project in order to establish the boundaries of the research, and they are outlined in the list below.

- The built collection system optimization model of HPP is developed based on deterministic data.
- The HPP plant is assumed to be located in India.
- Infinite land availability is considered for the location of the generating elements.
- The positions of the WTs and PV modules are determined by applying certain constraints, further explained in Section 3.2.1, but are not optimised.
- The power capacity or power rating of the HPP components are known.

- The average price of electricity in India and the discount rate are assumed constant during the whole period.
- One-year power time series of wind and solar with hourly precision are used in the problem and extrapolated for the entire lifetime of the HPP.
- Different clustering techniques, also referred to as strategies, are applied to the power time-series data of wind and solar during the first stage of the optimization process, which corresponds to the Investment problem, as it is explained in detail in Section 3.4.1. In order to reduce the computational time and complexity of the problem.
- Introduction of a constraint that allows the connection of each generation node uniquely to the PCC and to its 5 or 15 nearest generation units, depending on the study case.
- Assumption of a transportation power flow model.
- Power losses in cables are neglected in the problem formulation.
- Estimation of distance between each pair of nodes done by calculating the Euclidean distance between them in 2D.
- Location of the PV systems on the downstream side of the WTs to avoid potential wake effects.
- Overplanting is applied to increase the overall capacity factor of the HPP plant.
- Consideration of only active power when determining the cables capacities, omitting the reactive power contribution.
- Limited computational capacity resulting from the use of an Intel Core i5-8250U CPU running at 1.60 GHz with 8 GB of RAM machine.

CHAPTER 2

Literature Review

In order to assess the current state of the art on the problem of HPP collection system optimization, a thorough literature review is pursued. When performing such survey, due to the innovative character of the study, no previous literature can be found. However, the problem in question is in turn composed of several subjects that need to be investigated independently to shape the system as a whole and define its technical specifications. Therefore, data has been gathered about every one of them independently: PV systems, wind turbines, cables and electronic equipment such as inverters and step-up transformers, and the integrated HPP system. A review of the mentioned data is assessed in the following subsections.

2.1 Background on Hybrid Power Plants

Renewable energy technologies are becoming more and more popular as their validity as an electricity generation alternative to fossil fuels has been proved. Apart from the continuous cost reductions attained, the utilisation of these clean technologies entails a considerable abatement of greenhouse gas emissions. This can significantly help facing climate change and addressing the problems and conflicts associated to it.

HPPs in particular, exhibit certain benefits with respect to individual RES as such. Being the result of the combination of several power generation sources, they are able to compensate for some of the inherent drawbacks of renewable energies [8]. Among the latter, unpredictability, intermittency, lack of reliability and continuous availability of power. The integration of RES can ease the matching of supply and demand and reduce the grid instabilities, thus maintaining the voltage and frequency within their respective adequate levels. Furthermore, capital budgeting and investment planning metrics like the Net Present Value (NPV), can be increased, hence, enhancing profitability.

This energy generation solution is expected to play a key role in the imminent transition towards a more distributed generation system that allows the setting of a so-called smart grid, leaving behind the current centralised scheme [9]. In-

deed, research and development of Hybrid Renewable Energy Sources (HRES) are progressing, intending to make their operation resemble that of a conventional generation unit. One of the interests this encompasses is the greater adequacy of HPPs to grid code stipulations and market structures formulated when the share of fossil fuels prevailed over that of renewables.

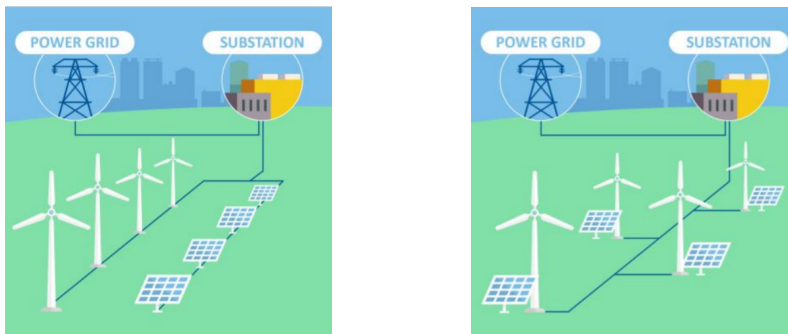
In this regard, the grid integration community has agreed that hereinafter, market structures will experience a transformation. As the share of renewables in the power system increases, meaning that low-cost energy is added to the power grid, the focus will be placed more on increasing revenue from capacity and adequacy markets rather than from energy markets [5]. A more detailed review can be found in Section 2.3. Thereby, even if more volatile and unpredictable renewable generation comes on stream, electricity supply will continue to meet demand.

Advances in certain areas of research have made it possible for the state of the art of hybrid plants to be what it is today [10]. More innovative and high-quality devices with higher conversion efficiency are becoming available in the electronics field, leading to the improvement of the system's reliability. Also, the lifetime of AC and DC gadgets is being extended. Consequently, the system's performance is enhanced and required maintenance work reduced due to the creation of tailor-made automatic controllers. Besides, functional simulation software for hybrid energy systems is emerging, and more and more optimisation software is developed and refined. It is also worth mentioning the continuous improvements that renewable technologies are benefiting from. For example, PV panels are seeing their efficiency increased by means of advances in the manufacturing process and improvement of the characteristics of the materials. On the other hand, modern wind turbines are increasingly cost-effective, powerful, reliable, and more affordable for power producers. As companies aim to build more sophisticated wind turbine technology, more refined tools are needed along the way.

Concerning the coupling of the HPP to the grid, it is made by a unique common connection point (see Figure 2.1, with the consequent advantage of installing a single substation, leading to a decrease in cost. Furthermore, there appears to be a possibility to oversize the rated capacities of wind and solar over the power capacity of the grid, meaning that the infrastructure use is exploited and power fluctuations smoothed.

Other matters of interest are the connection and HPP possible configurations. Four kinds have been identified as a function of the common integration and operation of the generating power sources, as illustrated in Figure 2.2. Essentially, all types allow maximising the use of the point of common coupling (PCC) with

the grid, by improving the capacity factor and reducing the capital expenditure and the permitting timing. Likewise, since the PV modules and wind turbines share site and are in close proximity, the proposed configurations are also beneficial during the resource assessment and site conditioning phases and considerably reduce the operation and maintenance costs (O&M). In addition, through their implementation, the optimisation of the sizing of the substation to the most probable range of output power becomes more straightforward, but curtailment needs to be carefully considered. The first configuration is the most used up until now, while the other three are still just potential alternative solutions [11].



(a) Same substation and grid connection. (b) PV panels integrated with the turbines.

Figure 2.1: Types of HPPS in terms of integration and operation of different generating modules.[11]

The first and most commonly deployed configuration consists of wind and solar co-location with shared substation and coupling point to the grid. An example can be seen in Figure 2.2.I. Among the advantages of this configuration, avoidance of PV panels shading by the WT blades, flexibility during development and sizing phases, and PV's capacity not limited by turbines' converters, are highlighted.

On the other hand, when PV modules are integrated at the wind turbine level (Figure 2.2.II.), the PV inverter can be eliminated and replaced by a hybrid converter sourcing AC & DC, since the WTG-coupled system leverages the already existing conversion device inside the WTs. This is achieved by connecting the PV to the converter of the WT. However, there are drawbacks to this setting: as opposed to the first-mentioned configuration, shading of the PV panels by the turbines' blades is a problem, which could be potentially solved by installing the panels further apart. Nonetheless, this can lead to the need of longer cables and, thus, higher costs and active and reactive power losses in the lines.

The third and fourth possible configurations (represented by configurations III. and IV. in Figure 2.2) are DC-Coupled solutions, which are characterized by a DC collector system to which the different generators are connected. For HVAC connected systems, i.e., configuration III., the presence of a grid-side inverter is required to transform the DC power extracted from each generation technology into AC power to be connected to the HVAC grid. Whereas for HVDC connected systems i.e., configuration IV., a DC/DC converter is used to couple the HPP plant to the grid.

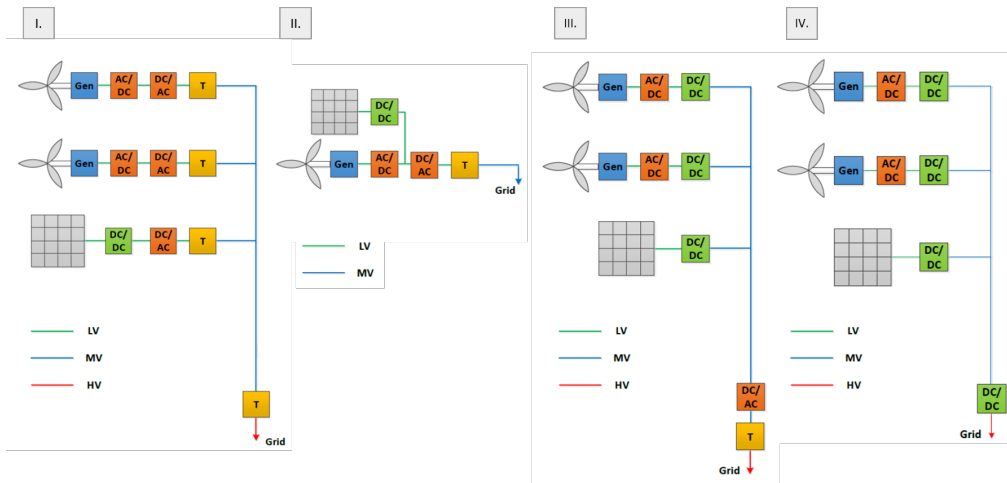


Figure 2.2: Configurations for: I. Co-Located HPP. II. WTG-coupled system integration. III. DC-coupled HPP for HVAC connection. IV. DC-coupled HPP for HVDC connection [12].

2.2 Advantages and Functionalities

As mentioned in previous sections, the deployment of HPPs offers several benefits compared to pure renewable technologies like wind or solar. Some of them are depicted in Figure 2.3.

In the first place, when installing wind and solar together, thanks to their negative correlation, i.e., complementarity, and varying generation patterns, the yearly capacity factor of the plant and the Annual Energy Production (AEP) increase. This can be translated into better exploitation of the electrical infrastructure and higher business case certainty, thus lower financing costs.

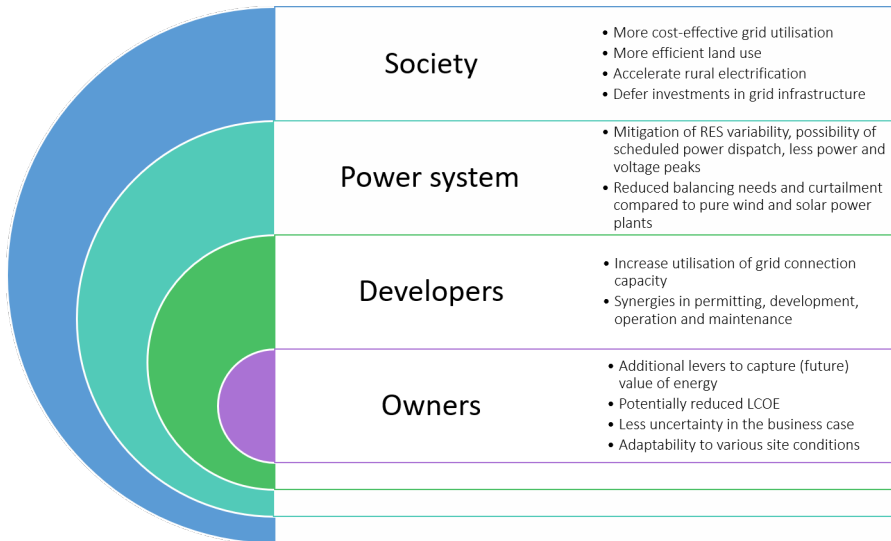


Figure 2.3: Foreseen benefits of wind-solar HPPs [11].

In addition, the power output stability is reinforced over time, thus leading to abatement of fluctuations and gradients, which is translated into an increased dispatchability, that ultimately eases the meeting of demand. Most interestingly, even when solar and wind are not correlated, HPP deployment results favorable. For example, if the electricity market price is negatively correlated to wind power due to a high share of wind, when prices are high, revenue can be obtained from solar energy.

Another interest derived from HPPs is the possibility of optimising the network use, achieved when developers install more capacity than the existing or authorised in the connection agreement. Although this decision can involve energy curtailment when generation exceeds the grid connection capacity, it is the preferred approach to take full advantage of the plant. Nevertheless, in [12] it is estimated that wind and solar PV can be over-dimensioned at least by 20% without incurring in energy curtailment. This is thus translated into savings in grid development (CAPEX reduction).

The possibility of sharing the balance of system costs (BOS), both hardware costs and soft costs, is also an important business driver behind HPPs. Savings obtained through hardware costs depend on the configuration itself and soft

costs are reduced when the technologies are built simultaneously. Among hardware costs, the transmission lines, power electronics e.g. shared inverters between technologies, and controllers, are the most significant. On the other hand, soft costs are related to permitting, interconnection, land costs, customer acquisition and labour.

In terms of Operation and Maintenance (O&M) costs, there can also be a substantial reduction since thanks to the joint development, the same technicians can carry out maintenance operations for both PV and wind systems.

As commented in the previous section, HPPs usually require establishing one unique connection point to the grid, commonly referred to as PCC. This leads to a reduction in infrastructure investment costs. Also, since the installed power and the energy output per square meter increase, the land is more efficiently used.

Regarding permitting procedures, developers can harvest synergies since combining the aspects mentioned above can help meeting the complex grid codes in less time and supporting the customer to enter into new markets or to operate the HPP even under challenging conditions.

Finally, HPPs can facilitate the electrification process of rural areas since they can provide more scheduled power dispatch to meet demand in certain regions characterised by weak power grids.

2.3 Market Opportunities

The economic potential drawn from an HPP not only depends on its resources and costs, but also on other aspects like market context and structure. In a potential future scenario dominated by renewables, where ancillary services and capacity markets are more relevant than the traditional energy market, the profitability of HPPs will most likely be better than that of the individual technology [5].

In the Capacity Market, power plants receive capacity payments as a function of the correlation between their capacity availability and the energy demand. By these means, system operators ensure that there is always the required capacity. However, as a consequence of their uncertainty and lack of reliability, renewables have hardly been able to take part in this kind of market. The development of HPPs is hence of interest, as they allow the inherent variability of RES to be reduced and production to be more constant, and thus easier to be scheduled.

Through the Ancillary service market, generators are paid for providing services to keep the stability and reliability of the power grid in the short term. These services generally include frequency and voltage control. Also in this case, renewables have traditionally had a low presence, but in the near future, a rise in their participation is intended to be promoted.

2.4 Power electronics topologies

Two possible configurations can be established when designing the topology of a grid-connected wind and solar photovoltaic (PV) hybrid power plant: AC coupled HPP and DC coupled HPP. The first two schemes in Figure 2.2 depict two possible configurations that present an AC coupled topology, whereas the two diagrams on the right, represent DC coupled topologies. In Section 2.5 a more detailed description of AC coupled configurations will be presented, alongside Figures 2.6 and 2.7.

When the decision is made to take an AC coupled topology, all subsystems have a point of common coupling on the AC side within the HPP. For the case of DC coupled HPPs, all technologies are connected to a DC bus. This requires the wind turbines to divide their actual functionality of fully rated converter into independent AC/DC inversion and DC/AC inversion.

The first mentioned topology exhibits the advantage of easier implementation compared to the latter. However, when selecting a DC configuration, better utilization of the electrical infrastructure is achieved. On the other side, the disadvantage of the DC is that it is currently in a nascent stage and requires new control architecture and algorithms.

Figure 2.4a depicts how in the AC configuration, the grid receives power directly from the output of DC/AC and AC/DC-DC/AC devices. In this case, there is no DC bus in the system [13].

In Figure 2.4b, it can be seen how the DC voltages at the output of the individual AC/DC and DC/DC units installed after the wind turbines, the PV panels and the batteries are then combined on the DC side and pass through a common DC/AC inverter before being connected to the grid. In the described topology, the role of the DC/AC inverter remains also the voltage control at the DC bus. Contrarily to individual electronic devices which can incorporate a maximum power point tracking (MPPT) system to get the maximum power from the electricity sources.

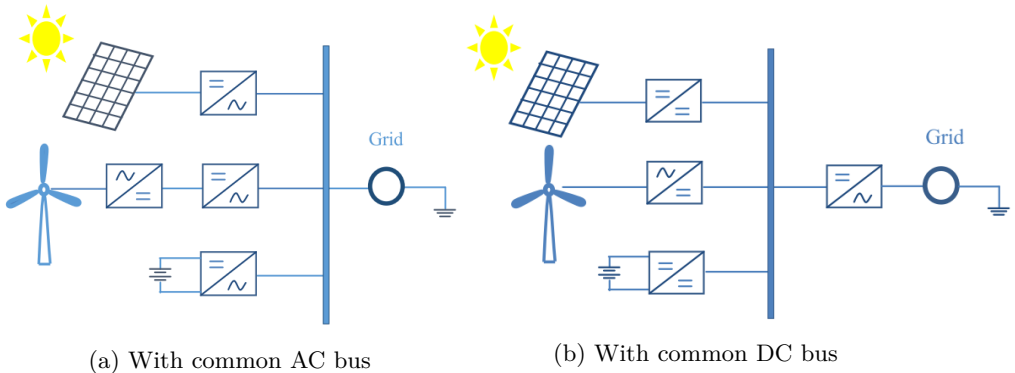


Figure 2.4: Grid-connected hybrid system [13]

2.5 Large scale photovoltaic power plants

2.5.1 Electrical components

The fundamental elements that compose a utility-scale PV plant, also referred to as Large Scale Photovoltaic Power Plant (LS-PVPP) have three main functions. They are, converting solar energy into electricity, connecting the plant to the grid, and ensuring adequate performance. These functions are respectively carried by the PV panels, PV inverters and transformers.

PV panels

The main components of an LS-PVPP are the PV panels. They consist of solar cells connected in series and encapsulated in a frame. They are responsible for capturing the sun's energy and transforming it into electricity, by the photovoltaic effect, that can be then delivered to the power grid customers. The PV effect is a semiconductor effect that causes the movement of the electrons of the PV cell when the light reaches it. The output power generated by a solar PV cell is in DC mode. The LS-PVPP contains many solar cells connected in modules and several modules forming strings that can be connected in parallel to produce the required DC power output.

Depending on the materials used, different PV cells can be distinguished. Currently, two main types of PV cell technologies are available in the market: crystalline and thin-film, and others that are not yet available but are emerging, e.g., organic cells made from polymers. The former have been more commonly used at a utility-scale level because of the higher stability, amount of land used, availabil-

ity of primary resource and mostly, as they present higher efficiencies (around 20%) when compared to thin-film that are a cheaper alternative and have efficiencies up to 15% [14]. Thin-film cells are a good alternative when the radiation and temperature coefficient are low. Crystalline silicon (c-Si) cells are subdivided into two groups: mono-crystalline silicon (mono-c-Si) and multi-crystalline silicon (multi-c-Si). On the other hand, three possible types of thin-film exist: Cadmium Telluride (CdTe), Copper Indium (Gallium) Di-Selenide (CIGS/CIS), and Amorphous Silicon (a-Si).

The selection of the material used to manufacture the PV modules plays a key role in the resulting occupied area by the LS-PVPP. Thus, better and improved materials enable to have smaller areas since more power per square meter is extracted. This also reduces both installation costs and cost of the land, which are two critical drivers when developing utility-scale PV projects.

Studies and acquired experience have demonstrated that the performance of the PV modules decreases over time as a consequence of degradation. The degradation pace depends directly on the environmental conditions, e.g. humidity, temperature, solar irradiation, and in that case is known as potential induced degradation (PID). But also, the materials used, their quality and the manufacturing process play an important role in the degradation rate. On this account, researchers are looking into new ways of enhancing the performance of the PV cells, with more efficient materials and characteristics that also lead to a decay in prices. In particular, at the utility-scale level, other cells characteristics are becoming crucial lately, i.g. CO_2 generation reduction during the lifetime of the cell, recyclability and sustainability [14].

PV inverters

Another vital element that affects the performance of large scale PV plants is the inverter. The PV inverters are electronic devices used to convert the DC power generated by the PV panels into AC electricity, for connection to the internal AC grid. They can be arranged either in central configurations or in strings, as depicted in Figure 2.7(a) and Figure 2.7(b), respectively. Many modules can be connected to one inverter, and they can be both arranged as series strings or parallel strings. However, for LS-PVPPs it is more suitable to install them according to a central configuration, as noted in Figure 2.5, both in terms of efficiency and power per area. This way, many modules are connected in series, constituting high voltage (HV) strings connected in parallel to the central inverter. This configuration offers more straightforward installation and higher reliability, at the expense of the lack of maximum power point tracking (MPPT)

per string, characteristic of string inverters.

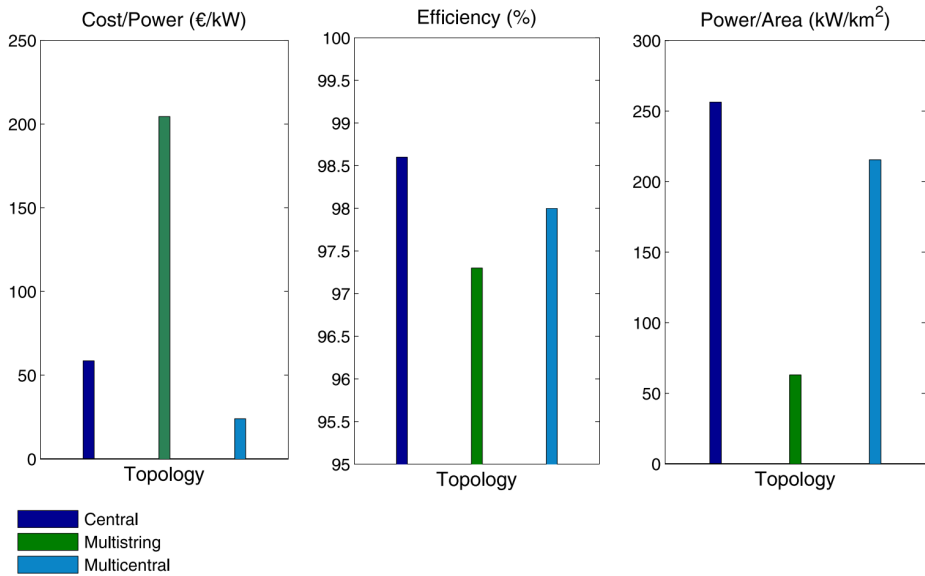


Figure 2.5: Comparison of market available PV inverter topologies for LS-PVPPs [14].

Apart from the aforementioned task, PV inverters perform other functions to maximise the plant's output. These range from the protection and isolation of the system from irregularities and grid or PV modules instability, to optimisation of the tension across the strings and functioning monitoring. PV inverters need to compensate for some issues related to their interconnection with the PV modules. In this respect, they are designed to have galvanic isolation for the leakage current coming from the modules. Moreover, inverters' disconnection is forbidden and the provision of grid support functions must be ensured, as well as voltage and frequency control and fault ride-through (FRT) capability. In addition, inverters must comply with the country standards and regulations. Finally, an MPPT tracker is required due to the non-linear characteristics of the intensity and voltage. In view of the current trend pointing towards power generation systems that perform more and more like conventional power plants, PV inverters have to improve considerably their operation and controllability.

Transformers

Step-up transformers are needed since, for LS-PVPPs, the output voltage of the PV modules and inverter is below the level of the HPP collection system. They take the power at the output of the PV inverter and raise its voltage to the required grid level, i.e., 25kV, 33kV, 38kV, or 110kV, depending on the grid connection and country electrical standards. Two main types can be found in solar PV plants, distribution and transmission transformers, depending on whether the desired voltage level is at the plant collection system or directly connected to the transmission grid. The latter requires even further voltage stepping up.

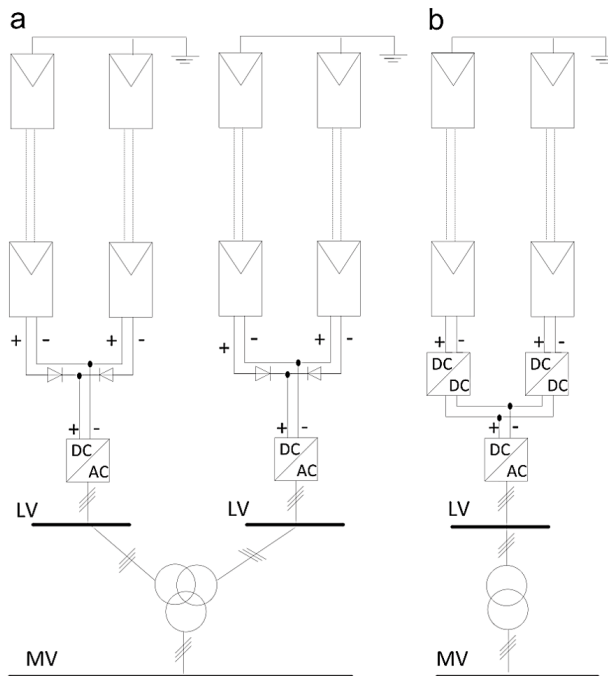


Figure 2.6: Connection of transformers at medium voltage. (a) Central PV inverter with three winding transformer and (b) multistring PV inverter with two winding transformer [14].

Another consideration is the power rating of the PV inverter. Article [14] points out that, if this is below 500 kW, the transformer used is a two-windings transformer, while if it is higher than 500 kW, the most commonly used transformer is the three windings transformer. Nonetheless, this article also reports that the

two winding transformers were the most used in the last decades. However, the development of central inverters with greater rating lead to the utilisation of improved transformers. Lately, for real LS-PVPPs, the three winding transformer is the most common as it allows to connect two central PV inverters. For the case of multi-string inverters, the best option remains the use of two winding transformers (Figure 2.6). Considering the rated power is relevant as it can have severe consequences for the LS-PVPP operation. A transformer with a rated power lower than the normal operating power of the plant could become a bottleneck. Likewise, if the rated power is too high, the global performance may be challenged. The selection is carried in any scenario according to the nominal power, but also to its cost and efficiency.

2.5.2 Internal PV plant configurations and topologies

When assessing the performance of an LS-PVPP, the internal topology is a key factor, which entails the interconnection of the PV modules, PV inverters and step-up transformers. Three basic configurations can be found: (i) central topology, (ii) string and (iii) multi-string, and a fourth one, the AC module integrated that has been studied but not yet implemented at utility-scale level. Figure 2.7 illustrates all the possible topologies mentioned.

The central topology is characterised by the connection of several thousands of PV modules to one unique inverter. These PV panels are clustered in hundreds of parallel strings containing hundreds of modules in series. Then, in the string topology, each PV string is connected to one inverter. Finally, the multi-string topology consists of the interconnection of one PV string to a DC-DC converter and then, around 4 or 5 DC-DC converters, linked to one inverter.

As a general rule, the central topology has been the preferred option in projects developed across the globe. This can be due to its simpler installation and the fewer components present in the overall plant, compared to the multistring inverter topology. The drawback of the latter is its complex installation and the large number of inverters installed, which combined, make this option less appealing to investors. However, they show higher efficiency levels thanks to MPPT control in each string; hence, more profound research on this matter should be effectuated.

All in all, the proper election of the plant's topology is of extreme importance, and this may also obey to the influence that the solar radiation and shading effect have on the power produced by the plant.

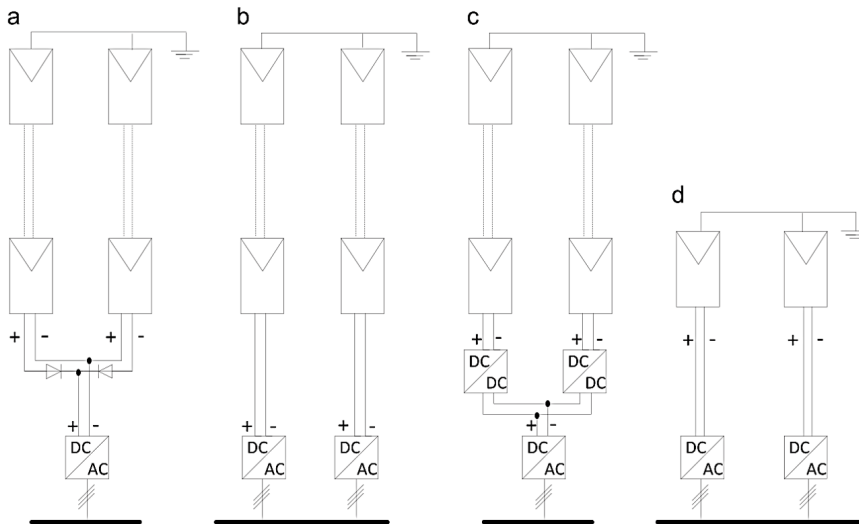


Figure 2.7: PV inverter topologies. (a) Central, (b) string, (c) multistring, and (d) module integrated [14].

2.6 Large scale wind farms

The present section focuses mainly on the electrical network design of onshore and offshore wind farms rather than on the technology itself. As reported in the Literature [15], it is estimated that the cost of the electrical infrastructure accounts for approximately 15–30% of the overall initial costs; thus the optimization of its design becomes of particular relevance.

When conducting the literature survey for the HPP collection system design problem, it is noted that in the past two decades, similar research was performed for onshore and offshore wind farms, and that thus becomes a valuable source of useful information. By virtue of the above, a comprehensive literature review of the methods studied so far for the optimization of the electrical cables in onshore and offshore wind farms is carried out. A detailed description of what was found relevant is explained hereunder.

2.6.1 WTs Collection System Design

According to article [16], there are several steps for the design and optimisation process of the collection system of wind farms. The starting point is the intro-

duction of the data, i.e. parameters, variables, objective and constraints. Several possibilities concerning these elements are identified. Variables can be integer, binary and continuous, and the parameters can be bounds or limits to the variables, unit costs, time-series data or technical characteristics of the technologies. Then, the next step is the choice of the network topology. A variety of options exist, from radial, radial plus star, radial plus star plus splices to single looped or other types. In any case, each topology should be designated together with the desired optimisation objective, i.e. Length (L), Investment (I), Investment plus Reliability (IR), Investment plus Losses (IL), and Investment plus Reliability plus Losses (IRL). Finally, the last stage encompasses selecting the solution method to apply: clustering, heuristics, metaheuristics, global optimisation or hybrids.

Clustering consists of splitting the WTs into subgroups, maximising the resemblance of the individuals included in the cluster and minimising it for those that belong to a different subgroup. Regarding heuristics, they are a fast technique, but the quality of the solutions they provide tends to be weak. However, when combining them with clustering, its limitations are reduced. Metaheuristic methods arise from the need to improve traditional heuristics to avoid limitations like falling into a local minimum. They provide better solutions with no certified optimality. Among the most popular, the following can be found: Genetic Algorithm (GA), Particle Swarm Optimization (PSO), Simulated Annealing (SA). Lastly, global optimisation techniques, also known as exact methods, provide certified optimal solutions for convex problems. They require the use of an external commercial solver, generally used as a black box, which implements algorithms like Branch-and-Cut or Benders Decomposition. They can be further split into: Binary Integer Programming (BIP), Mixed Integer Linear Programming (MILP), Mixed Integer Quadratic Programming (MIQP), and Mixed Integer Non-Linear Programming (MINLP). Finally, hybrid methods appear as the combination of different techniques, i.g. evolutionary algorithms and heuristic rules mixed with exact formulations.

Regarding the applicability of the methods, it is noted that problems focused on Total length (L), Investment (I), and Investment plus total electrical losses (IL) have been tackled with heuristics, metaheuristics, and global optimisation methods. While, when reliability is targeted, mathematical formulations are the preferred approach.

According to the literature, each method presents advantages and disadvantages and, as mentioned, is adequate depending on the purposes aimed. Many authors with different approaches have addressed the cable routing prob-

lem. Due to its intrinsic complexity and the high number of constraints needed for its formulation, many studies have opted for heuristics (i.e. [17], [18]). Metaheuristics are also the choice in some cases, such as [19], where the cable network optimisation problem is solved by utilising a Multiobjective Genetic Algorithm. Only a few preferred to use Mixed Integer Linear Programming (MILP) (i.e. [20], [21]). While, in some cases, the implemented technique was a matheuristic, which is the hybridisation of metaheuristics with mathematical programming. The hallmark of this method lies in the possibility of defining heuristics over a black-box MILP solver. As far as can be determined with the carried research, only three studies have taken power losses along the cables into account and are proposed in [22], [23] and [15]. Consideration of power losses makes it possible to optimise not only for minimising investment costs but also for minimising future revenue losses.

CHAPTER 3

Definition of model inputs

Solving the optimization problem requires collecting, filtering, and fitting different data. All the inputs needed to populate the equations and run the model, can be visualized in Figure 3.1. These data range from the technical specifications of both the generation technologies and the conversion and transmission equipment, through financial factors, prices and costs, to the layout configuration where all the nodes are previously located. The use of the mentioned data becomes more evident when going through the mathematical formulation in Section 4.3.

In the present section, the general characteristics of the data and the methodology conducted to define the model inputs are outlined. It is structured as follows: first, the technical specifications of the two RES are presented, followed by a description of the criteria used for their respective locations in the plant. Subsequently, the integration of both energy generation technologies in the site is carried out to constitute the HPP and aspects such as grid capacity are defined. Then, in the following subsection, the technical specifications of the conversion and transmission devices are described. Finally, other data necessary for the model are presented, such as the time series used, the price of electricity, the cost of the cables and the interest rate.

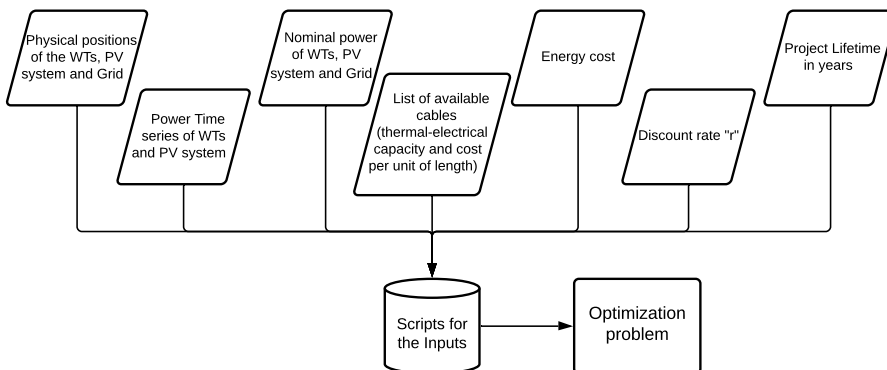


Figure 3.1: Inputs for the Optimization problem.

Apart from searching in the literature and benchmarking market available data, a model was provided as an additional data source [8]. The latter provides a sizing solution of the different technologies composing the HPP plant, from which some of the technical specifications of the energy sources are extracted. The model is used as a first approach for the estimation of the installed capacities of wind and solar PV, as a reference for various calculations and to escalate parameters needed along the way. These are described in detail throughout this section.

3.1 Generation technologies specifications

3.1.1 Wind turbines

The turbine model selected for the study is taken from the previously mentioned sizing model and is characterized by a rated power of 2.1 MW and a nominal voltage of 33 kV. The WT's lifetime, which is estimated to be 30 years, and technical specifications used for carrying out some necessary calculations are listed in Table 3.1.

Wind rated power	2.1 MW
Nominal voltage before step-up trafo	690 V
Nominal voltage with incorporated step-up trafo	33 kV
Rotor diameter	97 m
Hub height	120 m
Lifetime	30 years

Table 3.1: Technical characteristics of installed wind turbines.

3.1.2 Photovoltaic modules

Concerning the PV modules used to conform the PV system, they have been extracted from [24]. They present a nominal power of 245 Wp and voltage and current at maximum power of 30.2 V and 8.13 A, respectively. Their technical specifications can be found in Table 3.2.

Type	Multi-crystalline
Nominal power of PV panel	245 Wp
Voltage at P_{max} (V_{MPP})	30.2 V
Current at P_{max} (I_{MPP})	8.13 A
Dimensions	1650x992x40 mm
Module area	1.64 m^2
Operating temperature	-40 to +85 °C
Lifetime	25 years

Table 3.2: Technical characteristics of installed PV modules.

3.2 HPP configuration design

3.2.1 Layout definition

A major stage for solving the problem is the location and distribution of the turbines, photovoltaic panels and PCC. Therefore, the first step in the layout creation process consists of the definition of the WTs positions, respecting the separation criteria, and the PV systems positions and their internal configuration. Finally, all the aforementioned are integrated to constitute the HPP overall layout.

The wind turbines are organized according to a grid pattern. They are arranged in two parallel strings composed of 10 turbines each. There is a total number of 20 WTs in the HPP plant. Initially, the amount of turbines selected for the project was 62, value extracted from the given sizing model and the result of dividing the optimal wind installed capacity of 129 MW by the rated power of the WTs (2.1 MW). However, to reduce the system complexity and computational time, the number is decreased to 20 WTs. Therefore, the total installed capacity of wind reaches a value of 42 MW.

When defining the wind turbine layout, the aim is to avoid interrupting each other's wind profile and speed as a consequence of the wake effects. In order to do so, different distances are kept between the turbines, depending on the wind. As it can be seen in Table 3.3, the predominant wind direction in the HPP plant location is East. The turbines are thus distributed keeping a minimum safe distance of 8-rotor-diameter in the prevailing wind direction and 5-rotor-diameters in the perpendicular direction.

N° of WTs	20
N° of strings	2
N° WTs per string	10
Turbine spacing predominant wind direction (m)	8D
Turbine spacing in perpendicular direction (m)	5D
Predominant wind direction	East

Table 3.3: Considerations for design of WTs layout.

The procedure to establish the internal configuration of the PV modules is different from that of the WTs. The PV modules are strategically allocated in 400 parallel strings containing 50 PV modules connected in series, hence forming PV systems of 20000 modules. The output of the whole system presents a rated power of 4.9 MW, voltage of 1.5 kV (30.2 V multiplied by 50 modules in series), and current of 3.25 kA (8.13 A multiplied by 400 strings), as it can be seen in Figure 3.2. The output is directly connected to a central inverter to convert the DC voltage into AC voltage. This configuration is selected among all the solutions depicted in Figure 2.7, due to its simplicity and the possibility of connecting several thousands of PV modules to a unique inverter.

N° of PV systems	3 or 8
N° of PV modules per PV system	20000
N° of parallel strings in each PV system	400
N° modules in series per string	50
Spacing between panels (m)	1.95
PV panels orientation	south

Table 3.4: Internal PV system considerations.

In the model presented in Section 4.2, the generation units positions are used as nodes. However, for the sake of convenience, instead of establishing a different node for each PV panel, the junction node between the PV inverter and the PV system is selected. Contrarily to what is conducted for WTs, where each is represented by a node in the problem. Furthermore, two layout alternatives are evaluated in this study. The first encompasses the installation of 3 PV systems and the second of 8 PV systems. The ultimate objective is to evaluate the ben-

official effect of installing same power capacities of wind and solar PV, to obtain the utmost HPP potential and maximise yields.

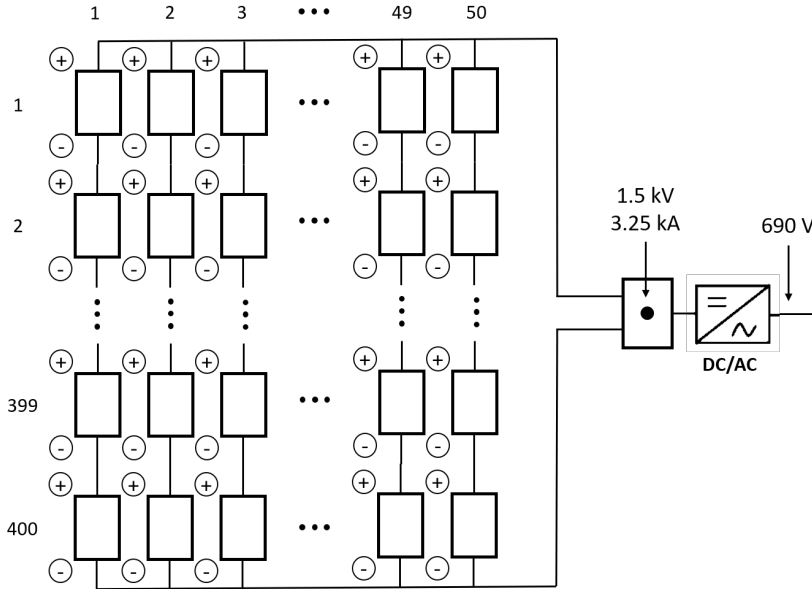


Figure 3.2: Internal PV system setup.

Analogously to the case of the wind turbines, the installed solar PV power is initially extracted from the sizing model. Since its value is significantly high, it can lead to extremely long computing times and excessive computational complexity. For these reasons, the total installed power is decided to be reduced.

Regarding the spacing between the panels, it is calculated by means of the equation in [24] that aims at determining row spacing to reduce inter-row shading and associated shading losses. It takes into account parameters such as the latitude and the dimensions of the PV module. The value of the latitude for India used for the calculation is 20.59° . The value obtained is 1.95 m and is established between both rows and columns.

In addition, in order to get the most from the solar panels, they must be orientated pointing in the direction that captures most sunshine. Since the HPP plant is placed in India, which is located in the northern hemisphere, the optimal orientation of the PV modules is south.

After defining the distribution of the two generation technologies independently, the HPP layout is settled. To start with, an assumption is made, consisting of establishing the PV systems on the downstream side of the WTs to avoid potential wake effects. Another aspect that needs to be taken into account when integrating the RES is the shadowing effect. In a wind-solar hybrid plant, WTs can cast shadows over the PV modules, incurring in energy generation losses, faults or modules damage caused by hot spotting. The former can be originated not only because of turbine towers shadows but also due to shadow flicker effect. The latter affects the PV power output as a result of intermittent light intensity.

The issue described leads to the definition of the empty zone concept. It is essentially the empty space left around the WTs required to achieve very low shadow losses. Results from the study [25], show that the value selected for the empty zone shall be comprised between the values of the safety and operating zones. Being the operating zone defined as the area devoted to maintenance work on the wind turbine, and the safety zone the area defined for keeping a safe distance from, e.g., public roads and highways, buildings, and living habitats.

The equations used for obtaining the values of the safety and operating zones, respectively, are 3.1 and 3.2.

$$\text{Safety zone} = \text{hub height} + 1/2 \cdot \text{rotor diameter} + 5 \text{ meters} \quad (3.1)$$

$$\text{Operating zone} = \text{rotor diameter} \cdot 1.1 \quad (3.2)$$

The input parameters needed for the calculations are listed in Table 3.1. According to those values, for the present project, the calculated safety zone is 173.5 m, and the operating zone is 106.7 m. The empty zone is hence estimated as 120 m, value comprised between the safety zone and operating zone values. Meaning that the PV systems are thus installed a minimum of 120 meters away from the turbines.

After taking into account all the considerations described above, two different layouts are finally generated. The resulting layouts studied in the project are represented in Figures 3.3 and 3.4.

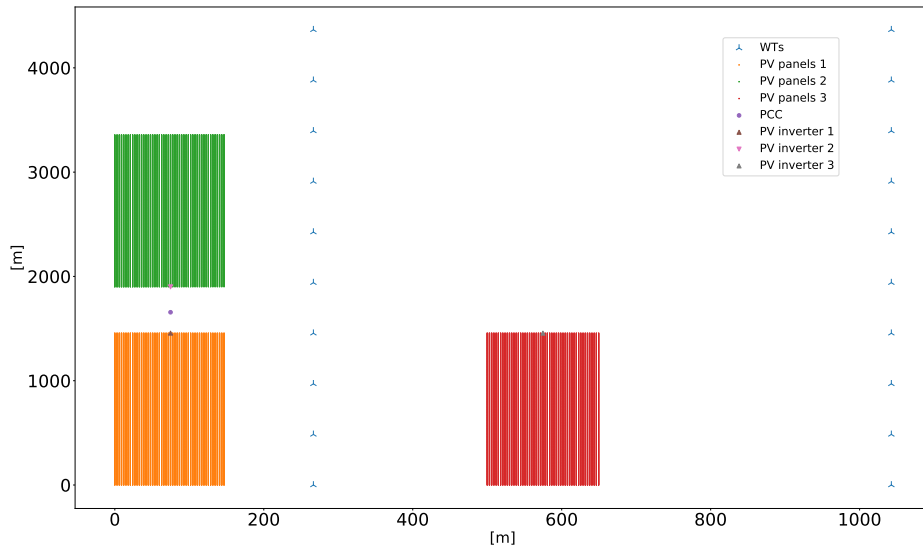


Figure 3.3: HPP layout 2 including 20 WTs and 3 PV systems.

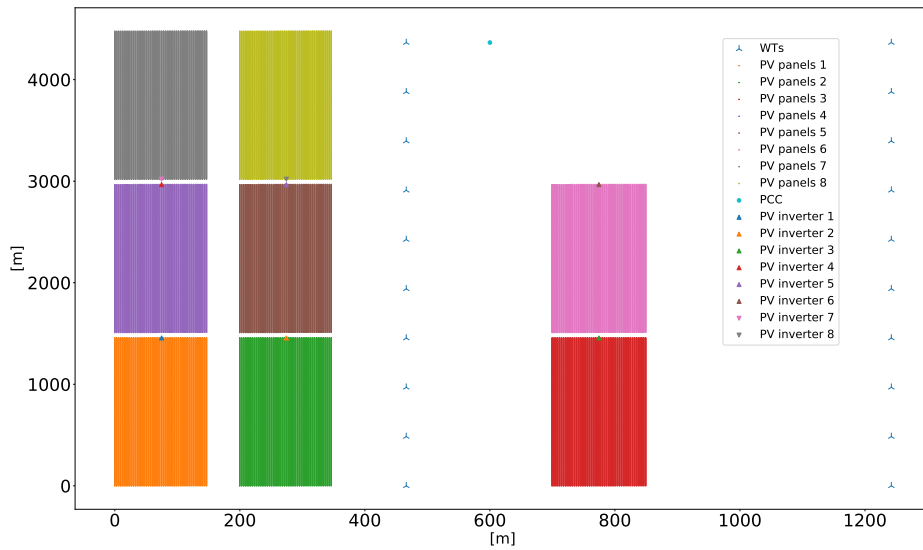


Figure 3.4: HPP layout 3 including 20 WTs and 8 PV systems.

Each HPP layout is analyzed for different study cases, hereinafter referred to as Tests, conformed by acting upon certain parameters, e.g., grid capacity and available cables. Figure 3.5 shows a diagram presenting the characteristics and parameters chosen to shape each of the above-mentioned Tests. It is worth mentioning that six tests and associated simulations have been conducted during the project, however, for the sake of conciseness, only three are presented and analysed in this thesis. All the selected combinations are introduced in the optimization model to obtain the optimal cable routing network and its associated cost, for each particular test. The purpose is to understand which is the best approach when designing the electrical infrastructure for a given scenario.

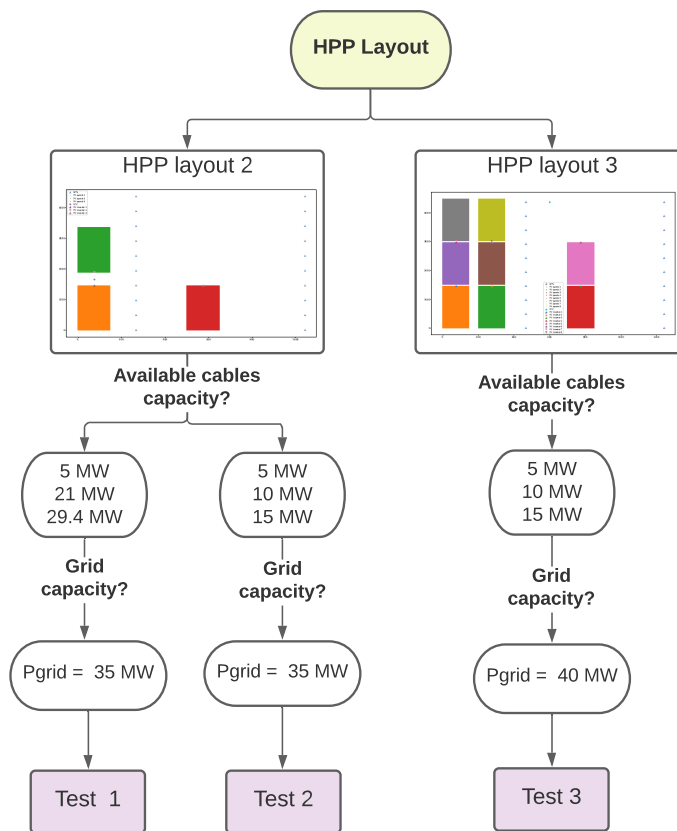


Figure 3.5: Procedure for establishing the set of Tests to be evaluated for the optimization.

With regard to the topology of the HPP, two options are contemplated. In the first alternative, the generators are connected at a voltage level of 690 V, meaning that the voltage level within the HPP is 690 V. They share a step-up transformer to elevate the voltage to 33 kV. The output from the transformer is then connected to the PCC. Whereas in the second possible topology, each technology presents a step-up transformer that increases the voltage from 690 V to 33 kV. In this case, the voltage level in the HPP plant is 33 kV. These two potential configuration are illustrated in Figures 3.7 and 3.6. For this project, it is decided to implement the second topology (Figure 3.6) following with what is commonly done in utility-scale wind and solar projects deployed all over the world. The viability of the first topology of shared step-up transformer, could be evaluated for future work by formulating an optimization problem. This analysis should take into consideration several aspects, e.g., transformer costs, and power losses incurred as a consequence of lower voltage in cables.

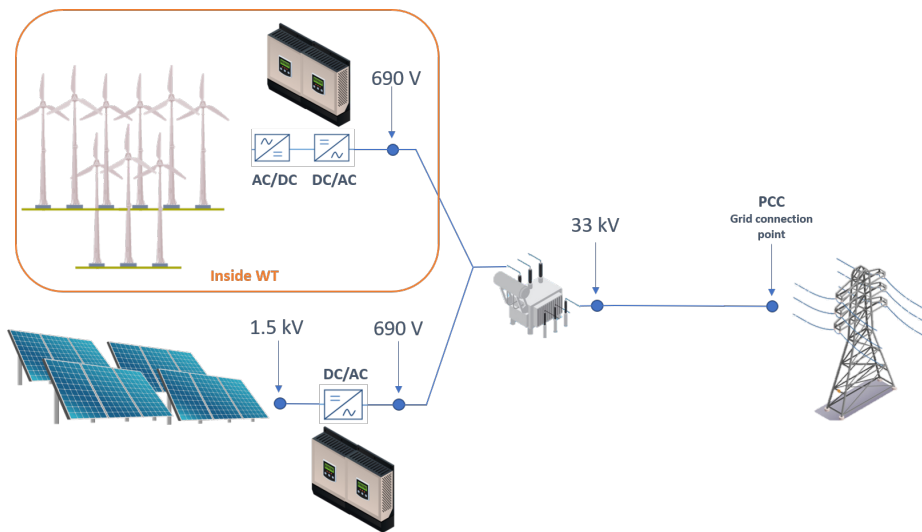


Figure 3.6: Configuration with individual step-up transformer per energy source.

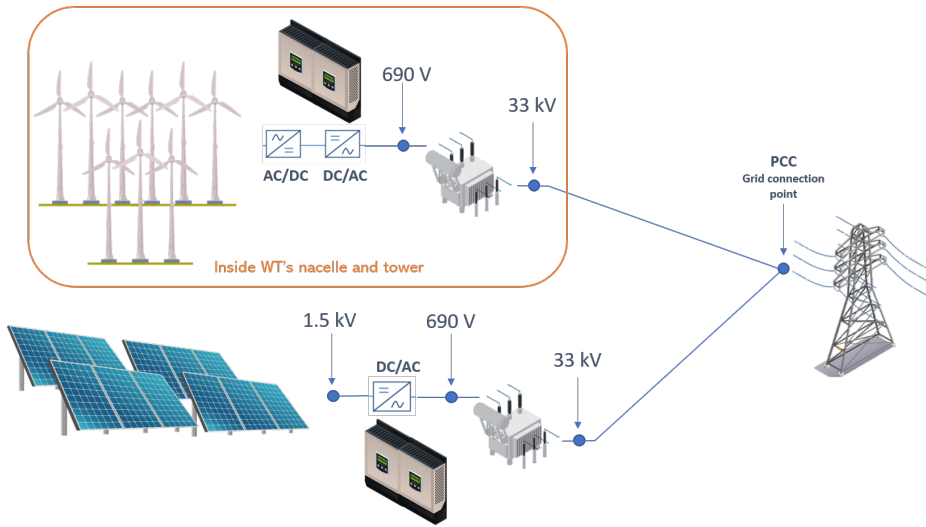


Figure 3.7: Configuration with shared step-up transformer for both energy sources.

3.2.2 Overplanting and Grid rated capacity

Traditionally, the electrical infrastructure (collection and transmission systems) design of wind farms has been done considering operation at nominal power. For the sake of simplicity, the variability of the wind was not taken into account. This approach ensures the system's robustness, which means it can withstand nominal power at all times. In addition, energy curtailment was not conceived, since generally, developers and plant administrators aim at maximizing the power supplied to be sold and made profit on. However, in some occasions, if supply exceeds demand the price of energy is negative, becoming thus necessary to incur in curtailment.

It was not until a decade ago that the importance of wind variability was questioned and better understood, leading to the emergence of a new concept known as overplanting. The over dimensioning of the HPP plant consists of installing more RES capacity than the grid connection's. This practice of overplanting arises because during most of the time the electrical infrastructure is unused, since the capacity factors of wind and solar are 30-40% and less than 20%, respectively [26]. Indeed, it rarely happens that nominal power operation is achieved. The idea behind this new tendency is to increase the generated power when wind and solar generation levels are low by setting more turbines and PV modules, and

contrarily, curtailing energy when the resources allow providing nominal power. The purpose is to exploit the resources more efficiently to generate power close to the evacuation capacity for maximizing the revenue, smoothing variability and increasing capacity earnings. Indeed, there is a clear distinction between the contracted capacity, which corresponds to the maximum amount of AC power that can be delivered to the PCC, i.e. the maximum capacity that can be scheduled, and the actual installed capacity. This should be possible as long as the total exported power does not exceed the contracted one.

According to the Indian example found in [27], the RES installed capacity is overdimensioned by 50%, doubling the grid connection capacity. Following this example and the criteria applied in the sizing model provided, and then escalating it to the problem of study according to installed wind and solar PV levels, three possibilities are defined for the HPP grid connection capacity. In the first place, when installing 20 WTGs of 2.1 MW of nominal power (resulting in a total value of 42 MW) and 1 PV system of 4.9 MW, the grid power is set to 30 MW. On the other hand, for the same amount of wind capacity and 3 PV systems (meaning 14.7 MW in total of solar PV), the grid connection capacity becomes 35 MW. Besides, for the third studied configuration that comprises 20 WTs (42 MW of installed wind) and 8 PV systems (39.2 MW of installed solar power), the value of the grid rated capacity is established at 40 MW.

3.2.3 Lifetime

The technical lifetime of a power production plant is the expected time, in years, during which it can operate with a performance close enough to its standards. Many factors influence the lifetime duration of the plant, i.e., the number of usage hours, and may decrease its efficiency slightly over the years. At the end of its technical lifetime or after it reaches a poor performance level, the plant is decommissioned or must undergo significant renovations to extend its operation. Currently, a lot of effort is put into research and development of wind and solar PV technologies with the aim of achieving higher efficiencies and longer lifetimes.

When determining the overall lifetime of the HPP, it is vital to assure that the technologies that compose it can withstand operation for the whole period considered. Therefore, for the present study the HPP lifetime is 25 years, due to the fact that the PV modules lifetime is 25 years and the lifetime of the wind turbines is 30 years. The value selected is the most restraining of both. These specifications are taken from the provided sizing model for the Indian case and the technical datasheet of the PV modules.

3.3 Energy conversion and transmission equipment specifications

Exhaustive benchmarking is conducted to select the market available cables, inverters and transformers that best suit the needs of the designed HPP.

3.3.1 Cables

Initially, the cables used for the project and their technical characteristics are extracted from [15]. However, as the study is developed, it becomes clear that the incorporation of new cables with lower capacities (5 and 10 MW) is beneficial. Table 3.5 illustrates the collection of the selected market available cables.

Cables	Type	N. of WTs supported
		2-megawatt
cb01	1	7
cb05	1	10
	2	14

Table 3.5: Basic information on the real-world cables used for the HPP collection system.

As it can be noted, the cable capacities are given as a function of the number of wind turbines they connect. Moreover, the number of WTs each cable can support is given for 2-megawatt WTs; however, the nominal power of the turbines installed in the HPP plant is 2.1 MW. It is assumed that for this case, this criterion can be also applied without posing any issue. The resulting capacities of the cables are thus, 14.7 MW, 21 MW and 2.4 MW, respectively.

The capacities of the complete assortment of cables available for the project, considering the additional cables of 5 and 10 MW, are depicted in table 3.6. Depending on the characteristics of the Test assessed, a different combination of cables is used.

The incorporation of a new 5 MW capacity cable arises when analyzing the base case, in which each generation technology is connected to the grid through an independent collection system, operating at its rated power. This value is chosen since the nominal power of the PV systems is 4.9 MW. This way, it is ensured that each of them is directly connected to the PCC through an independent feeder.

Cable capacities (MW)				
5,	10,	14.7 \simeq 15,	21,	29.4

Table 3.6: Capacities of cables used in the project.

The cables of 10 and 15 MW are included as a last resort after running the model and observing that for the installed powers and the established grid capacity, the cables are overdimensioned since the power flows do not require cables with such high capacities.

3.3.2 Inverters

For the selection of the PV inverters, there is a broad range of criteria to be considered. The project capacity is one of the main drivers since it influences the inverter connection concept. In the present study, central inverters are chosen because the power level is on the megawatt scale and also due to the fact that the PV modules orientation and specifications are assumed to be the same. Therefore, there is no need to install string inverters with multiple MPPT. Another fundamental aspect that needs to be taken into account is the desired input and output voltage levels. The modules in the PV system are arranged in 400 parallel strings, containing 50 modules connected in series, leading to output voltage and current of 1.5 kV and 3.252 kA, respectively. Therefore, the inverter needs to be selected according to those specifications. Indeed, high-efficiency inverters must be sought. The additional yield often more than compensates for their higher cost.

After considering all the above-mentioned criteria, the model chosen is the SUN2000-215KTL-H0 from Huawei. It presents an input voltage level of 1500 V and an output voltage level of 690 V. This is an advantage since the voltage level after the wind turbines is also 690 V, which means that regarding the step-up transformer, two possibilities exist, as it is further explained in Section 3.2.1. A positive aspect of this model is its high performance, which is greater than 98.6%.

3.3.3 Transformers

The output power from the inverters usually requires a further step-up in voltage. The primary function of the transformer is to increase the voltage value to one that is suitable for the transmission of the energy produced to the connection point. It is thus responsibility of the step-up transformer to rise the voltage to the required AC grid level, i.e., 25kV, 33kV, 38kV, or 110kV.

The choice of the voltage level within the HPP plant is essentially a question of economy. Nevertheless, for plants where the transmittable power is within the order of dozens of megawatts, the voltage level of the system is often medium, i.e., 1 kV up to 35 kV. Therefore, a voltage of 33 kV is established inside the HPP.

Besides, as mentioned in previous sections, the voltage at the output of the PV inverter is 690 V, as is the turbine's output voltage. The selected transformer is hence one that elevates the voltage from 690 V to 33 kV.

The turbines generate power at a low voltage level, i.e., below 1 kV. Concretely in this project, at 690 V, so generally they are equipped with a transformer that steps up the voltage from the generator level to a medium voltage below 36 kV. Through this approach, each generation technology has its transformer, and the junction of the two is thus conducted at a medium voltage of 33 kV. There is another possibility that involves the connection of wind and solar generators together at low voltage level of 690 V, with the subsequent sharing of the step-up transformer, used to bring the tension to 33 kV.

3.4 Data collection

3.4.1 Power time series

The time-series data for wind and solar power are the average series of the measurements taken from 2 locations in India. They contain the time series of wind and solar generation measured with hourly resolution for the period from September 1, 2018, to October 31, 2019. The data is filtered and the values corresponding to 1 year, i.e. 8760 hours, are extracted, finally leading to a period between September 1, 2018, to August 31, 2019. The time-series are given for installed capacities of wind and solar PV power of 100 MW each. They are therefore normalized and scaled to the actual installed power of the HPP. Since three different cases are studied in this project, one for 20 WTs (42 MW) and 1 PV system (4.9 MW), one for the same number of WTs and 3 PV systems (14.7 MW) and one for also 20 WTs and 8 PV systems (39.2 MW), the data series are normalized three times, correspondingly.

Figures 3.8, 3.9 and 3.10 plotted below illustrate the wind and solar PV power series for the above-mentioned cases.

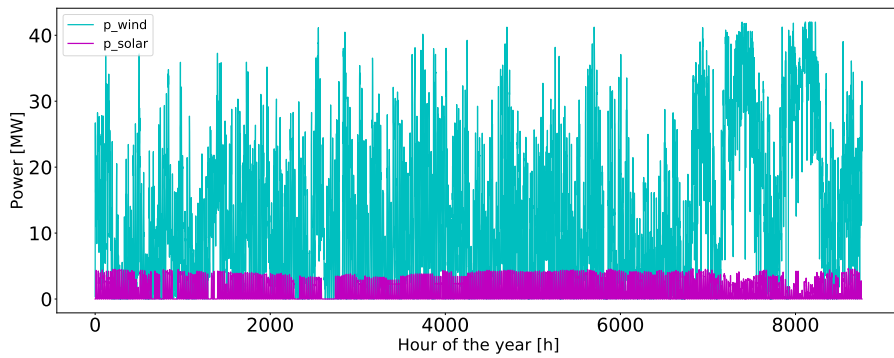


Figure 3.8: One year solar and wind time series normalized for 20 WT and 1 PV system.

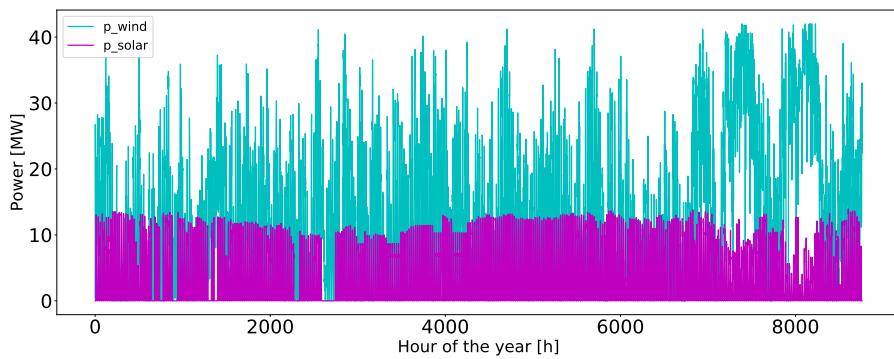


Figure 3.9: One year solar and wind time series normalized for 20 WT and 3 PV systems.

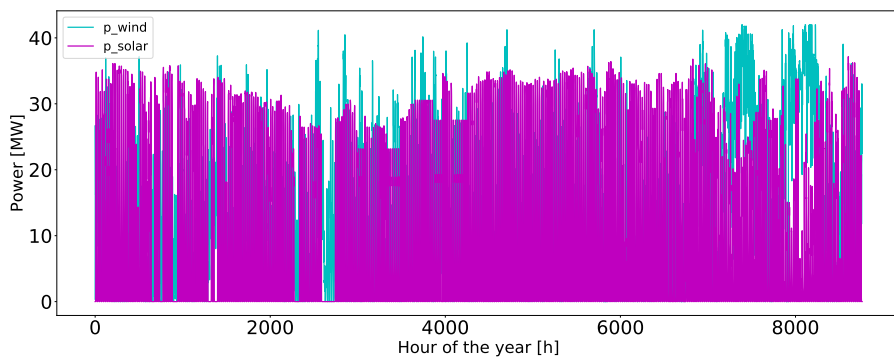


Figure 3.10: One year solar and wind time series normalized for 20 WT and 8 PV systems.

As previously mentioned in subsection 1.2, in order to simplify the computational complexity of the optimization problem, it is necessary to reduce the size of the complete time series by applying various clustering strategies. It is clear that this also leads to a considerable reduction of the model accuracy; therefore, at the time of establishing the strategies, those that are more representative must be applied. It is decided to proceed with four strategies that best capture the different possible cases, one for nominal power, one for average generation values, one for peak production values and one for low generation. In addition, a Base Case is also defined.

Strategy 0

In this strategy, the generating nodes, both turbines and PV systems, operate at their respective nominal powers (2.1 MW and 4.9 MW).

Strategy 1

Most realistic strategy, it intends to highlight the negative correlation between both technologies. Consists of defining an average production value for each month, taking into account only the relevant hours for each technology. In the case of wind, it is decided that these hours are those between 20h and 8h. While for solar, the range of relevant hours is 6h to 18h.

Strategy 2

Strategy built to reflect a high generation scenario. The peak values of each month are taken and assumed constant throughout the month.

Strategy 3

Aims at illustrating a case where production levels for each month are low. To do so, for wind, it chooses the values corresponding to the 25-percentile and, for solar, the values corresponding to the 50-percentile.

Base Case

A base case is defined to represent a scenario in which the collection systems of both technologies are designed independently. The traditional way used so far is applied, which consists of dimensioning the cables for the most demanding and conservative case, in which the generation technologies operate all the time at nominal power. The purpose of evaluating a base case is to assess the profitability of designing the electrical collection system for each energy technology separately, against the solution proposed in this thesis of a shared electrical infrastructure for both energy generation sources.

3.4.2 Cables Costs

The mathematical model used to estimate the capital expenses of the cables is extracted from [28]. This equation is widely used, and it is displayed below:

$$C_t = A_{p_t} + B_{p_t} \cdot e^{\left(\frac{C_{p_t} S_{n_t}}{10^8}\right)^2} \quad (3.3)$$

Here, C_t stands for the cost of cable type $t \in T$, given in €/km, being T the set of cables available. A_{p_t} , B_{p_t} and C_{p_t} are the coefficients of the cost model and are dependant on the nominal voltage V_n of the cable, as can be seen in Fig. 3.11.

V_n [kV]	A_{p_t}	B_{p_t}	C_{p_t}
22	$0.284 \cdot 10^6$	$0.583 \cdot 10^6$	6.15
33	$0.411 \cdot 10^6$	$0.596 \cdot 10^6$	4.1
45	$0.516 \cdot 10^6$	$0.612 \cdot 10^6$	3
66	$0.688 \cdot 10^6$	$0.625 \cdot 10^6$	2.05
132	$1.971 \cdot 10^6$	$0.209 \cdot 10^6$	1.66
220	$3.181 \cdot 10^6$	$0.11 \cdot 10^6$	1.16
275	$4.181 \cdot 10^6$	$0.07 \cdot 10^6$	0.66

Figure 3.11: Cables cost coefficients.

The unit cost is also based on S_{n_t} , which is the rated apparent power of cable t in VA and depends as well on the line to line voltage level. For the present project, a power factor of 1 is assumed and thus,

$$\cos \varphi = 1 \quad (3.4)$$

This means that the nominal apparent power (S_{n_t}) is equal to the nominal active power (P_{n_t}).

Besides, since the voltage level is 33 kV, the values of A_{p_t} , B_{p_t} and C_{p_t} used in the calculation are $0.411 \cdot 10^6$, $0.596 \cdot 10^6$ and 4.1, respectively.

3.4.3 Electricity prices

The responsible for the HPP development is considered a price-taker since cannot influence the electricity price and therefore has to accept it.

The electricity price is used in the mathematical model in order to quantify the cost of the energy that is curtailed instead of being sold to the power grid. According to the Electricity Market Report of December 2020 [29], for the case of India, it takes a value of USD 99/MWh, which corresponds to 82€/MWh.

Even if the electricity prices are fluctuating and reflect the electricity demand trend, it is assumed fixed for the whole lifetime of the HPP.

3.4.4 Interest rate

The debt interest rate r , namely the value used to reflect the capital costs of a project, is a required input used in the objective function of the optimization problem. It depends on the risk associated with the investment phase of the project and the source responsible for the funding. In the present study, it is used to compute the Net Present Value (NPV) of the HPP along its lifetime.

In [30], for the period of 2018 to 2030, for land-based wind and utility PV plants, the debt interest rate is forecasted to have a value between 4 and 5%. Hence, for this project, it is assumed to be 4.5%.

CHAPTER 4

Collection System Design

4.1 Problem description

The design of the electrical collection network of an HPP entails the optimal interconnection of the wind turbines, PV system and Grid that guarantees the minimization of the initial investment and the curtailed energy along the lifetime of the plant. The former comprises both the capital cost and the installation cost of the cables. The electrical losses have been excluded from the model due to their minor impact on the optimization model.

Following what graph theory describes for wind farms and applying it to the present case, the HPP can be represented by a tree graph with the root on the Point of common coupling (PCC) with the power grid. The topology proposed presents a radial configuration as it is the most common practice, since the inclusion of closed loops can incur in issues when it comes to cable sizing, even if the reliability of the system increases [23].

A deterministic approach for modelling cables is selected, considering exclusively radial layouts, due to the fact that for collection systems (33 kV of rated voltage), contrary to transmission systems (with voltage levels of the order of 110 kV and higher), it is often done this way.

It is well known that the process of designing the radial cable layout is considerably complex. As a matter of fact, finding the global optimum of this problem is classified as NP-hard in terms of computational complexity [15]. Meaning that its solutions can be verified in polynomial time. Regarding the different methods that can be adopted to tackle the problem, four big clusters stand out. They are as follows: heuristics, metaheuristics, global optimization with mathematical formulations, and hybrids, such as matheuristics [23].

Several options exist within the Global optimization category for modelling the cable routing problem. The current project is an example of MILP problem as it is more extensively described in Section 4.2. After completion of the problem's formulation, the solution can be found through an external commercial solver. In particular, the chosen MILP solver is the branch-and-cut solver implemented in

IBM ILOG CPLEX Optimization Studio V20.1.0 [31].

As detailed in Section 3, several cable types with different unit costs and capacities are considered in the model. Thus, optimization also needs to be done for the most suitable cable selection. Furthermore, given that the cost of the cable increases with its capacity, the one presenting the lowest price while meeting the requirements will be optimal.

A critical step in the design process of an HPP is the location of its main components: the PV modules and wind turbines. These have been previously determined in Chapter 3.2.1, and are assumed fixed throughout the optimization problem. The coordinates where the generation sources are located are used to calculate the distances between the nodes, which are inputs to the mathematical model. The estimation of the distance between each pair of nodes is done by calculating the Euclidean distance between them, in 2D. Apart from the already cited elements, the cost functions and the different scenarios also act as inputs to solve the problem.

The optimization problem can be divided into two stages: the Investment problem and the Recourse problem. The scheme in 4.1 is used to illustrate the ensemble of phases followed in the optimization process. At first, the model is run with the CPLEX solver, by introducing the resulting power values estimated from the application of each clustering technique, as many times as defined strategies. By doing so, the solutions of the investment variables for each strategy are obtained, resulting in the optimal designs of the collection layout. Then, for the next stage of the optimization process, namely the Recourse problem, the complete data series containing one-year hourly power values are used. In addition, the values of the binary investment variables calculated in the first subproblem are assumed fixed and introduced in the model. Thereby, the problem becomes linear since it only contains continuous variables and thus, easier to solve. The CPLEX solver then provides the values of the flow and curtailment variables for the given layout. As well as the optimal solution, which represents the investment cost, plus the cost of the curtailed energy.

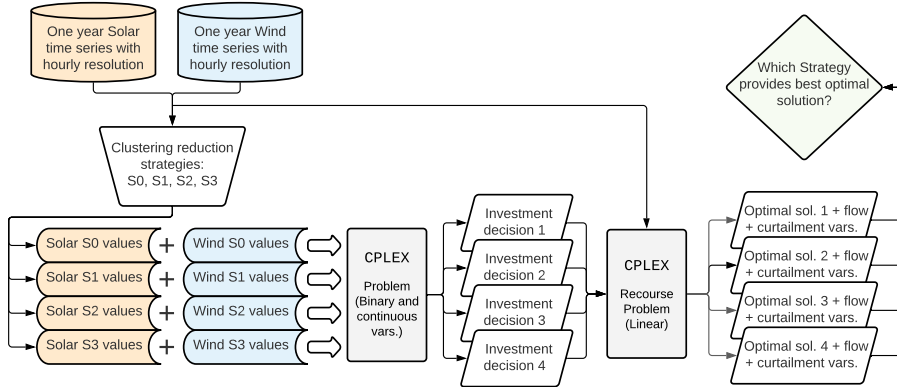


Figure 4.1: Collection system Optimization process: flow diagram.

4.2 Graph and model representation

The formulation of the optimization problem encompasses the design variables, non-design input parameters, constraints and objectives, as well as the global architecture of the algorithms used and the followed workflow. In the present section, the Mixed Integer Linear Programming (MILP) model is described. Its formulation has been carried out by defining in the first place the decision variables and the objective function and then by adding some real-world constraints to the problem. It is defined as a MILP due to the presence of binary and continuous variables.

When formulating the mathematical model, two possibilities exist. It is decided to go for a flow approach over the hop-indexed method for two main reasons [23]. The first being the existence of two generation sources with different rated power, which prevents from using the maximum permitted current of the cables and utilizing instead their maximum allowed power. And secondly, the greater flexibility and versatility achieved in the modelling process, allowing the inclusion of energy curtailment, which is used in this case.

The optimization aims at designing the cable routing of the HPP collection system for linking together the n_{WT} wind turbines and the n_{PVinv} PV systems (output nodes of each PV inverter) to the grid node (n_G). Concurrently, for each wind turbine and PV system, a power evacuation route is defined to model the possibility of energy curtailment.

A Set \mathcal{V} is defined and divided into three different subsets: containing the WT nodes $\mathcal{V}_{\mathcal{T}}$, the grid position node $\mathcal{V}_{\mathcal{G}}$ and the nodes of the PV inverter $\mathcal{V}_{\mathcal{P}}$. Let the nodes set be $\mathcal{V} = \mathcal{V}_{\mathcal{G}} \cup \mathcal{V}_{\mathcal{T}} \cup \mathcal{V}_{\mathcal{P}}$, where the element $h \in \mathcal{V}$, such that $h = 0$ corresponds to the PCC, $\mathcal{V}_{\mathcal{T}} = \{1, \dots, n_{WT}\}$ are the nodes of the WTs and $\mathcal{V}_{\mathcal{P}} = \{1 + n_{WT}, \dots, 1 + n_{WT} + n_{PVinv}\}$, the nodes of the PV systems. The grid node is considered the root of the distribution network, for it collects incoming arcs, while the nodes from the WTs and PV system are the generation nodes. All nodes $h \in \mathcal{V}$ have associated coordinates in the plane and have been previously used to calculate the Euclidean distance d_{ij} between the positions of the points i and j .

All these inputs are then combined to form a weighted undirected graph $\mathcal{G}(\mathcal{V}, \mathcal{E}, \mathcal{D})$, where \mathcal{V} is the vertex set, \mathcal{E} represents the set containing all available edges arranged as a pair-set $[ij]$, where $i \in \mathcal{V} \wedge j \in \mathcal{V}$. Finally, \mathcal{D} is the set of associated Euclidean distances for each member $[ij] \in \mathcal{E}$.

Additionally, let \mathcal{T} be a predefined list of different market available cables $t \in \mathcal{T}$ that can be used to connect each pair of nodes. Where for each type of cable $t \in \mathcal{T}$, \mathcal{K} represents the set of their respective capacities (k_t) sorted in ascending order and measured in megawatts and \mathcal{U} the set containing the cost per unit of length of each cable type defined by u_t . For every type of cable t , $k_t \geq 0$ and $u_t \geq 0$.

Once the graph representation is described, the model can be formulated. The Objective function presents two main components: the Investment costs (cables capital cost and installation costs) and the cost of the curtailed energy in each generation source. The costs of the inverter and the transformers are not included in the objective function because these two are inherent parameters from the selected models. They have fix values, and therefore, as they cannot be acted upon, they are not subject to optimization. Conversely, the Net Present Value (NPV) of the generated energy must participate in it to capture the system's operation. The possibility of energy curtailment would otherwise force the model to always propose the least possible production, leading to the dimensioning of smaller and, thus, cheaper cables. Since the energy curtailed is wasted, there is a crucial need to minimize it throughout the plant's lifetime.

In order to consider the presence of several generation states, a set Ω is introduced. It initially contains 8760 scenarios, one for every hour of the year. However, for the sake of simplicity, these scenarios are clustered. When strategy 0 is applied, the number of scenarios is reduced to 1. On the other side, when applying strategies S1, S2 or S3, the scenarios are clustered into 12, one per month of the year.

These are characterized by $\omega \in \Omega$, being the nominal generation scenario $\omega = 0$, representing the case where each power source operates at their rated capacity. Scenarios $\omega = 1$ to $\omega = 12$ capture the generation's time series for wind and solar for each month. It is worth mentioning that the inclusion of scenarios in the model adds significant complexity as the problem becomes a multi-period planning problem.

In the model, two continuous variables f_{ij}^ω and δ_h^ω are used in order to represent the energy that flows from node i to node j and the curtailed power in node h for scenario ω . In addition, two binary variables are included, $x_{ij,t}$ and y_{ij} , and they are described below:

$$x_{ij,t} = \begin{cases} 1 & \text{if edge}[i,j] \text{ is constructed with cable type } t \\ 0 & \text{otherwise.} \end{cases} \quad [i,j] \in E, \quad t \in T \quad (4.1)$$

$$y_{ij} = \sum_{t \in T} x_{ij,t} \quad [i,j] \in E \quad (4.2)$$

y_{ij} depicts whether the edge[i j] has been constructed with any kind of cable.

In addition, parameter P_h^ω is defined so the power produced in node $h \in V$ for scenario ω is characterized. For the cases where $h \in \mathcal{V}_T$ and $h \in \mathcal{V}_P$, as these represent generation nodes where power is produced, $P_h^\omega > 0$. Regarding P_G , it stands for the rated power of the grid. Thus, the amount of power sent from the energy sources to the grid cannot exceed this predefined value. This leads to the definition of the above-mentioned variable δ_h^ω that is used to depict the energy curtailed in node h .

Finally, there are cases in which, non-tree or disconnected solutions can be obtained. For instance, when electricity prices are low, curtailing energy could be more advantageous. It becomes therefore necessary to introduce some "dummy" variables and parameters to the model, to avoid these unfavourable situations. The aim is constraining the formulation to only provide solutions that exhibit a tree topology, where all the nodes are connected. These dummy parameters and variables do not influence the Objective function, and thus, do not modify the optimal solution. In order to consider them, the inclusion of a "dummy" scenario is also required. Subindex d is used to characterize whether a variable and a parameter is "dummy". This leads to the definition of $P_d^{\omega_d}$, a virtual power generated in each node being assigned a very low value. And $f_{ij}^{\omega_d}$, that stands for the "dummy" flow that circulates through the cables in the scenario "dummy".

4.3 MILP Model

4.3.1 Objective function

Once the graph representation of the problem has been defined, the model formulation is presented.

The Objective function is illustrated in the equation 4.3, where two main elements can be distinguished.

The first accounts for the cost associated to the initial Investment, which is computed as the sum of the cables' costs installed in each edge $[ij]$. It comprises the capital expenditure of cable t and its installation cost.

The second term represents the reliability represented by the cost of the curtailed energy at node h , for scenario ω and year μ . Thus, it evaluates the economical loss incurred throughout the entire lifetime of the HPP (given by parameter m) resulting from undispached power. For its calculation, the cost of electricity (c_e) in [$\text{€}/MWh$] and the discount rate r in [p.u.] are also used.

$$\min \left[\sum_{[ij] \in E} \sum_{t \in T} u_t \cdot d_{ij} \cdot x_{ij,t} + \sum_{\mu=1}^m \sum_{h \in V_T \cup V_P} \sum_{\omega \in \Omega} \frac{\delta_h^\omega \cdot c_e}{(1+r)^\mu} \right] \quad (4.3)$$

Modifications can be implemented in the Equation if different objectives are aimed. For instance, if only the initial investment optimization is targeted, the second component of the formula needs to be zeroed. If otherwise, the minimization of the total length of cables without their associated costs is aimed, the second term can be cancelled out, and the parameter u_t disappears from the Equation. These lead to simpler problem formulations.

When designing the model with the flow approach, as it is mentioned in the previous section, a formulation with edges is chosen over arcs. This implies that it is very hard to incorporate losses in the objective function. Despite this limitation, and even though the arc formulation would allow to include the losses in a linearized way, this procedure is preferred as the inclusion of power losses would result in an increase of the model's complexity.

4.3.2 Constraints

The following Equations are defined to represent the equality and inequality constraints of the mixed-integer linear optimization problem.

$$\text{s.t.} \quad \sum_{t \in \mathcal{T}} x_{ij,t} = y_{ij} \quad \forall [ij] \in \mathcal{E} \quad (4.4)$$

$$\sum_{i \in \mathcal{V}: i \neq h} \sum_{\omega \in \Omega} f_{hi}^{\omega} - f_{ih}^{\omega} + \delta_h^{\omega} = P_h^{\omega} \quad \forall h \in \mathcal{V}_{\mathcal{T}} \cup \mathcal{V}_{\mathcal{P}} \quad \forall \omega \in \Omega \quad (4.5)$$

$$- \sum_{t \in \mathcal{T}} k_t \cdot x_{ij,t} \leq f_{ij}^{\omega} \leq \sum_{t \in \mathcal{T}} k_t \cdot x_{ij,t} \quad \forall [ij] \in \mathcal{E} \quad \forall \omega \in \Omega \quad (4.6)$$

$$\sum_{h \in \mathcal{V}_{\mathcal{T}} \cup \mathcal{V}_{\mathcal{P}}} (P_h^{\omega} - \delta_h^{\omega}) \leq P_G \quad \forall \omega \in \Omega \quad (4.7)$$

$$\sum_{i \in \mathcal{V}: i \neq h} (f_{hi}^{\omega_d} - f_{ih}^{\omega_d}) = P_d^{\omega_d} \quad \forall h \in \mathcal{V}_{\mathcal{T}} \cup \mathcal{V}_{\mathcal{P}} \quad (4.8)$$

$$\sum_{i \in \mathcal{V}: i \neq h} f_{ih}^{\omega_d} = P_d^{\omega_d} \cdot (|\mathcal{V}_{\mathcal{T}}| + |\mathcal{V}_{\mathcal{P}}|) \quad \forall h \in \mathcal{V}_G \quad (4.9)$$

$$- P_d^{\omega_d} \cdot (|\mathcal{V}_{\mathcal{T}}| + |\mathcal{V}_{\mathcal{P}}|) \cdot y_{ij} \leq f_{ij}^{\omega_d} \leq P_d^{\omega_d} \cdot (|\mathcal{V}_{\mathcal{T}}| + |\mathcal{V}_{\mathcal{P}}|) \cdot y_{ij} \quad \forall [ij] \in \mathcal{E} \quad (4.10)$$

$$\sum_{[ij] \in \mathcal{E}} y_{ij} = |\mathcal{V}_{\mathcal{T}}| + |\mathcal{V}_{\mathcal{P}}| \quad (4.11)$$

$$0 \leq \delta_h^{\omega} \leq P_h^{\omega} \quad \forall h \in \mathcal{V}_{\mathcal{T}} \cup \mathcal{V}_{\mathcal{P}} \quad \forall \omega \in \Omega \quad (4.12)$$

$$x_{ij,t} \in \{0, 1\} \quad \forall [ij] \in \mathcal{E} \quad \forall t \in \mathcal{T} \quad (4.13)$$

$$y_{ij} \in \{0, 1\} \quad \forall [ij] \in \mathcal{E} \quad (4.14)$$

$$f_{ij}^{\omega} \in \mathbb{R} \quad \forall [ij] \in \mathcal{E} \quad \forall \omega \in \Omega \quad (4.15)$$

$$f_{ij}^{\omega_d} \in \mathbb{R} \quad \forall [ij] \in \mathcal{E} \quad (4.16)$$

Constraint 4.4 imposes that for each edge $[ij] \in \mathcal{E}$ built between two nodes i and j , only one kind of cable t can be used.

The flow conservation is depicted by Constraint 4.5. It states that the energy flow that enters a node (f_{ih}^{ω}) added to the amount of power generated at that

node (P_h^w) must be equal to the sum of the exiting flow (f_{hi}^w) and the energy that is curtailed at it (δ_h^w). Note that this constraint is not imposed to the node $h \in \mathcal{V}_G$, as it corresponds to the grid, where power is not produced.

On the other hand, the inclusion of Constraint 4.6 ensures that for any scenario, the power flow through a cable does not exceed its corresponding capacity. This restriction is composed of two subconstraints, as the flow f_{ih}^w can be negative or positive depending on its direction. If f_{ih}^w is positive it means that the flow goes from node i to node j , and if it is negative, from j to i .

In addition, Constraint 4.7 aims to illustrate that if the total amount of power produced in the generating nodes, for each scenario, is greater than the grid rated power, the excess of electricity needs to be curtailed.

Regarding equations 4.8, 4.9 and 4.10, they are implemented to guarantee that the cable connections can uniquely follow a tree topology with the root established in the PCC. The first one depicts the dummy flow conservation. It imposes that in the dummy scenario, for each WT and PV system node, the sum of power flows entering the node must be equal to the sum of flows exiting it, added to the dummy power generated on it. By applying the second Constraint, it is ensured that the grid receives the sum of all the dummy powers generated in the turbines and PV system nodes. Lastly, the third equation is used to illustrate that the dummy flow that can be supported by any installed cable has to be equal to the capacity of the smallest cable, i.e. if all generators were connected in series to a cable, that cable could withstand the total dummy power.

Finally, Constraint 4.11 ensures that the total number of edges is strictly the same that the number of generating nodes. Thus, it is guaranteed that the energy leaving a generating node must be supported by a single cable.

It is also worth noting that, unlike offshore wind farms, in onshore cases, cable crossing is not discouraged in application, indeed, it can be beneficial to reduce the investment costs incurred when installing parallel cables [7]. Therefore, no restrictions have been applied on this regard.

The mathematical model presented in this section, along with the inputs described in Section 3 are used to obtain the optimal solutions of the tests, whose results are presented in Section 5.

CHAPTER 5

Results and Discussion

As described in section 3.2.1 and illustrated in Fig. 3.5, diverse tests are run to evaluate the behaviour of the model and the solutions it provides under each configuration, originated from the combination of a certain layout with other selected parameters, i.e., grid capacity and cables capacities. The evaluated cases have been assigned different names, these being tests 1, 2 and 3. Two main analysis points are highlighted: the comparison between the results from the integrated optimisation and the optimisation for wind and solar independently, and the comparison between the results obtained when applying the different clustering strategies.

The computational tests presented in this section have been carried out on an Intel Core i5-8250U CPU running at 1.60 GHz and with 8 GB of RAM. Regarding the solver, the IBM ILOG CPLEX Optimization Studio V20.1.0, has been used. In order to control the termination of the MIP optimization, the relative MIP gap tolerance is set to 0.001 (i.e., 0.1%). The purpose of defining this parameter is to instruct CPLEX to stop the optimization as soon as it has found a feasible integer solution proved to be within 0.1% of optimal.

5.1 Test 1

As seen in Figure 3.5, Test 1 corresponds to the case where 3 cable types of capacities 5, 21 and 29.4 MW are available, 3 PV systems are installed and the rated capacity of the grid is established at 35 MW.

As described in Section 4.1, the optimization problem has two stages, the Investment and the Recourse problems. The optimal solution of the whole optimization corresponds to that of the Recourse problem, since it represents the integration of the investment cost of the cables and the cost resulting from the energy curtailed.

From Table 5.1, it is noted that the best optimal solution is obtained when applying strategy S1. This means that taking into account the negative correlation of wind and solar PV results beneficial, due to the fact that the sum of the investment cost, and the cost associated to curtailed energy, shows the lowest

value of all.

Strategy	solution_value	solution_value2
	Investment	Recourse
S0 nominal	€ 140,392,134.10	€ 25,026,193.87
S1 average	€ 11,134,534.73	€ 21,055,920.05
S2 peak values	€ 126,201,071.42	€ 21,272,270.93
S3 low values	€ 9,921,368.92	€ 57,014,492.16

Table 5.1: Optimal solution results for Test 1.

Based on the result from S0, it can be observed that the solution of the Investment problem leads to the discard of a considerable amount of energy. This being mainly due to the nominal power operation of the generating nodes, which provide a total power of 56.7 MW, higher than the grid's 35 MW capacity. This results in the optimal solution reaching a value of approximately 140 M€. Subsequently, the generated layout is introduced in the model along with the power time-series, resulting in a considerable decrease of the curtailed energy, due to the lower power values (using the nominal power as a reference).

Strategy S2 reveals a similar trend to that of strategy S0, since it uses peak generation values that are slightly lower than the nominal values, thus incurring in a marginally lower amount of discarded energy.

Finally, results obtained while running strategy S3 display a different pattern. Indeed, in the first-stage problem, the cables are dimensioned considering low power values in the generating nodes. Moreover, since the total power produced does not exceed the grid limit, there is no energy curtailment. Nevertheless, when the second-stage problem is run with the layout obtained in the previous problem in conjunction with the real-time series, since these are higher than those of strategy S3 and the installed cables do not have enough capacity, the curtailed energy rises considerably. As in can be appreciated also in Table 5.1, this results in a significant cost value.

The resulting collection system networks obtained by each strategy are illustrated in Figures 5.1, 5.2, 5.3 and 5.4. It is observed that for strategy S0 (Figure 5.1), PV systems in nodes 21 and 22 are connected directly to the PCC, and do not share the electrical infrastructure with the WTs.

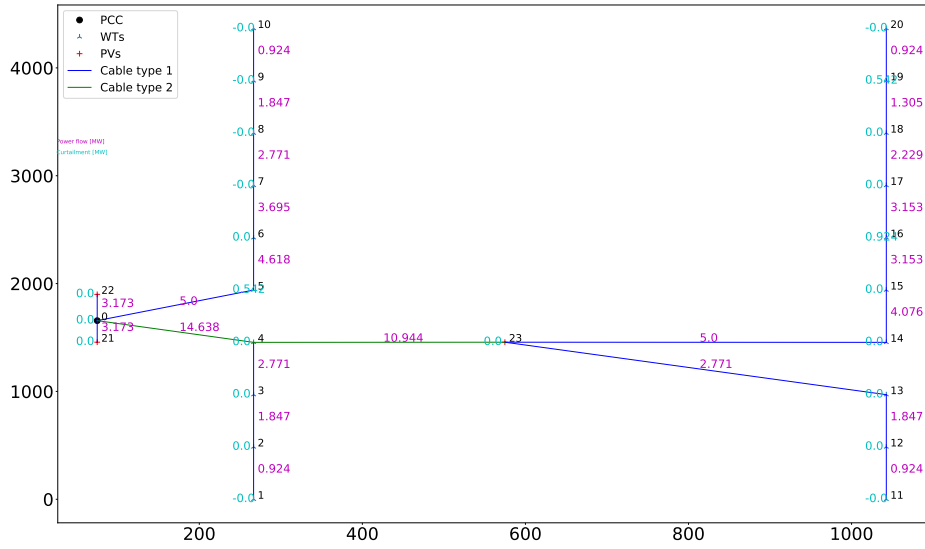


Figure 5.1: Optimal collection system layout when applying strategy 0 to Test 1.

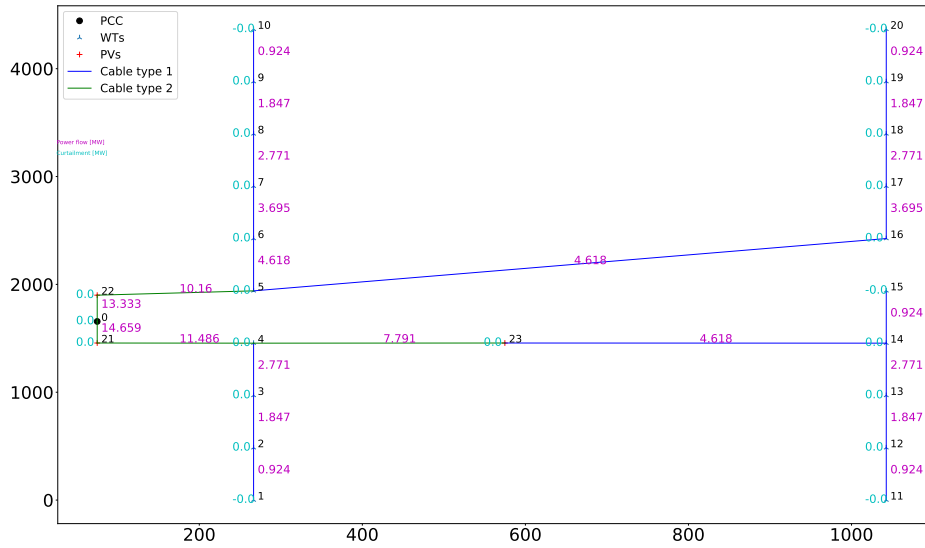


Figure 5.2: Optimal collection system layout when applying strategy 1 to Test 1.

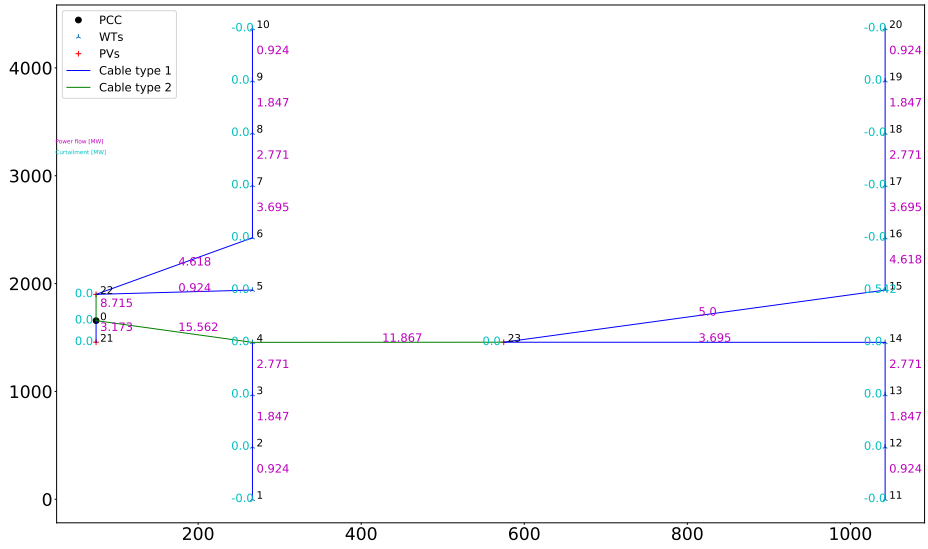


Figure 5.3: Optimal collection system layout when applying strategy 2 to Test 1.

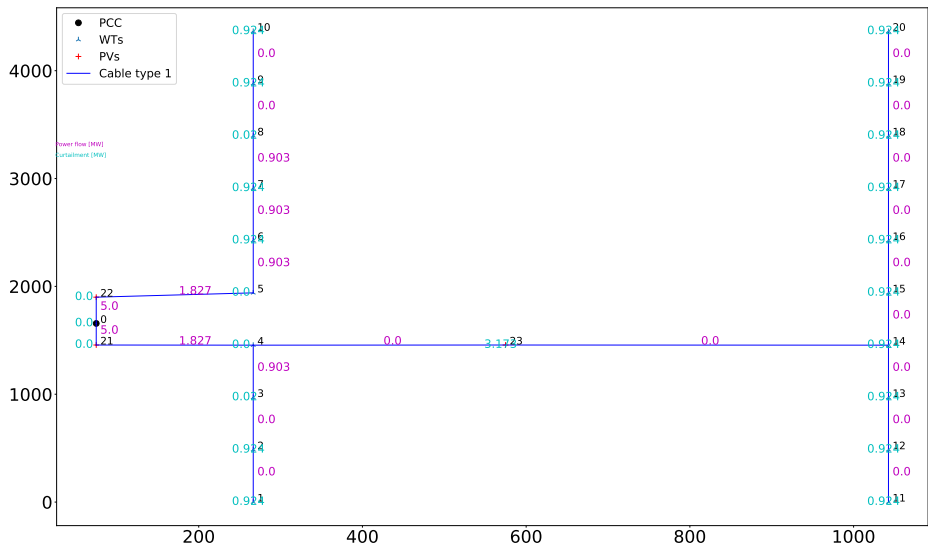


Figure 5.4: Optimal collection system layout when applying strategy 3 to Test 1.

5.2 Test 2

The next studied test, namely Test 2, also consists of 3 PV systems, 20 WTs and a grid rated capacity of 35 MW, although it differs from Test 1 in the available cables. For the present test the cables capacities are lower, these being 5, 10 and 15 MW, and they adjust better to the actual installed power of the HPP. The consequence is a reduction in the value of the best optimal solution, which is also achieved by means of strategy S1. The results obtained in Test 2 are listed in Table 5.2, and present a similar behaviour to those from Test 1.

Strategy	solution_value	solution_value2
	Investment	Recourse
S0 nominal	€ 140,294,721.06	€ 29,563,520.05
S1 average	€ 10,613,970.39	€ 20,600,466.41
S2 peak values	€ 125,965,525.92	€ 21,054,239.47
S3 low values	€ 10,173,399.76	€ 57,266,523.00

Table 5.2: Optimal solution results for Test 2.

The results from the implementation of strategies S0 and S2 perform the same way as they did in the previous test. Concerning the investment problem, also known as first-stage problem, they exhibit very high values, that are then reduced when running the model with the power time-series. Again, strategy 3 shows the worst performance, since it underdimensions the cables, thus leading to high values of curtailed energy. Strategy 1, provides an optimal solution value which is even lower than the value calculated in Test 1. It can therefore be concluded that it is worthwhile to select cables with capacities large enough to withstand the required power flow without incurring in oversizing, i.e., to match the installed power level of the plant.

5.3 Test 3

The configuration corresponding to test 3 is the most relevant as it is the one that most accurately depicts an HPP plant. The reason is that the installed capacities of wind and solar present similar values (42 MW and 39.2 MW, respectively), and the grid capacity value is set at half of the total installed capacity (40 MW, compared to a total installed power of 81.2 MW). Regarding the cables, three different types are available, with capacities of 5, 10, 15 MW, being adequate for the power level of the plant.

In Table 5.3, it is observed that the result from strategy S1 is significantly lower than the values obtained from the other strategies. This certainly shows that, in terms of profitability, taking into consideration the negative correlation of the generating technologies is advantageous.

Strategy	solution_value	solution_value2
	Investment	Recourse
S0 nominal	€ 259,527,253.62	€ 47,104,251.01
S1 average	€ 14,152,950.43	€ 28,518,115.08
S2 peak values	€ 232,938,096.14	€ 46,898,109.11
S3 low values	€ 11,273,282.03	€ 89,970,859.34
Base Case	€ 14,324,182.50	€ 35,764,540.41
Base Case PV in series	€ 15,825,764.74	€ 48,382,644.33

Table 5.3: Optimal solution results for Test 3.

In addition, strategy S1 presents the lowest change from the provided solution when running the model with the clustering strategy, with respect to the solution obtained for the whole data series. This gives an idea of the accuracy of the clustering technique, whose data is a much better representation of the real time-series data. It is thus desirable to use more realistic power values for determining the cables to be installed, rather than dimensioning them based on the nominal power ratings of the generators, as it is done with strategy S0 and similarly, with S2. The S1 approach leads to less energy curtailment. Moreover, the capacities of the main feeders in the electrical collection system generated with strategy S1 are more efficiently exploited than those generated through strategy S0 and analogously with S2, as it can be appreciated in Figures 5.6 and 5.5.

The practice that is most strongly discouraged is that of sizing for very low generation values (strategy S3), since for all the tests, it results in very high costs (see Tables 5.1, 5.2 and 5.3). The reason behind is that the cabling is designed considering that the generation nodes produce small amounts of power. However, when the selected cabling is run with the actual power series, the cables do not have sufficient capacity and a very high amount of energy has to be discarded. This curtailed energy has a huge associated cost.

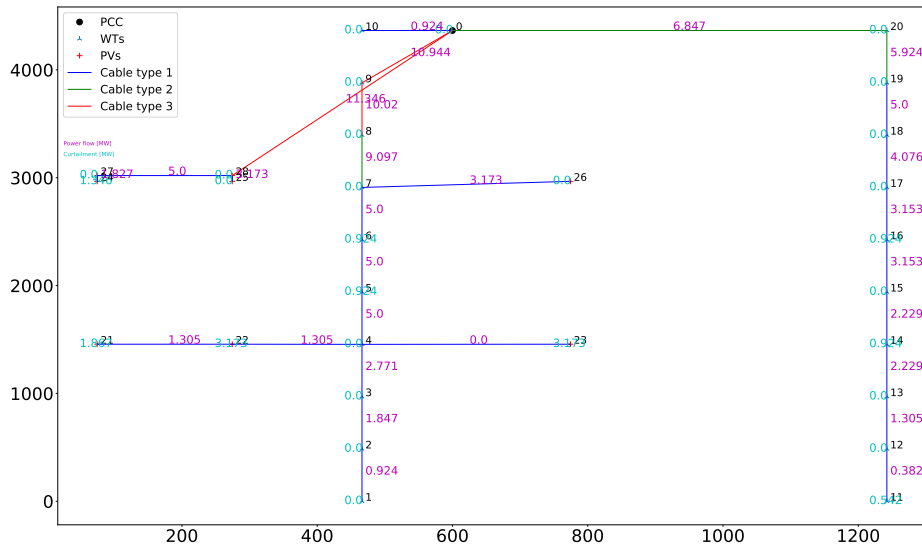


Figure 5.5: Optimal collection system layout when applying strategy 0 to Test 3.

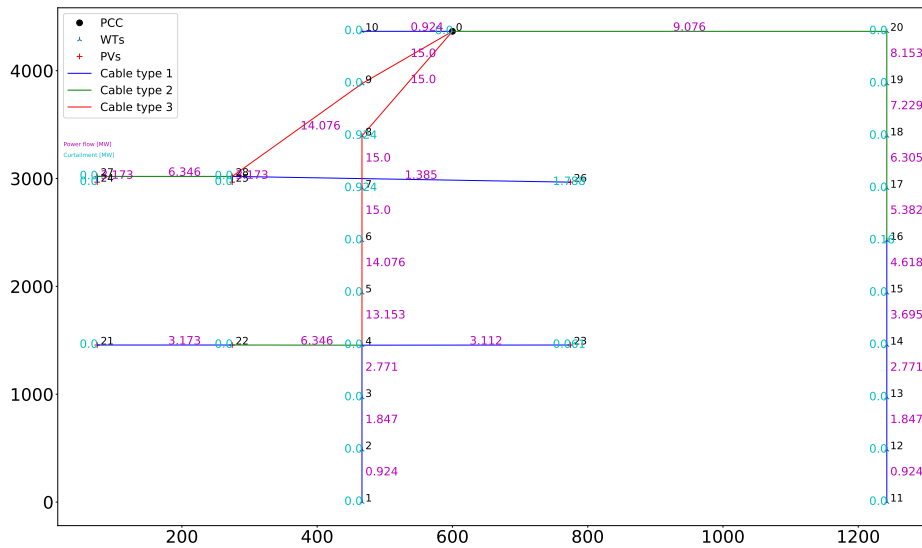


Figure 5.6: Optimal collection system layout when applying strategy 1 to Test 3.

After having analysed the strategies explained above, two variants of the Base Case are studied. The optimisation problem is run only with the WTs, providing a network. Then, the PVs are connected directly, without performing any optimisation. In the first studied case, each PV system is forced to be directly connected to the PCC, while in the second case, the PV systems are connected in series among each other and then connected to the PCC. The two alternatives are depicted in Figures 5.7 and 5.8.

Particularly, implementing the latter alternative results more expensive than connecting each PV system directly to the PCC. In both cases, the solution values depicted in Table 5.3 are worse than those obtained with strategy S1, confirming that the approach of establishing a common electricity infrastructure for both generation technologies is much more cost-effective and beneficial.

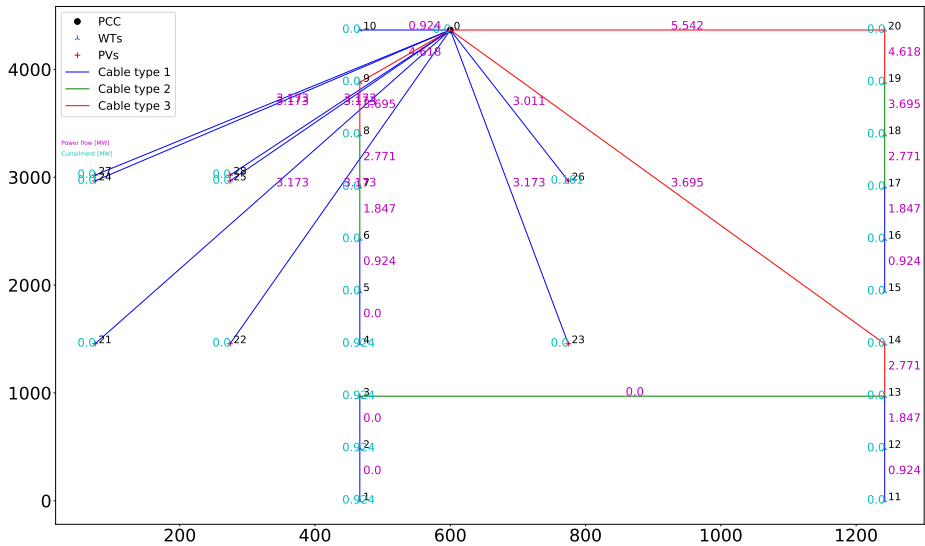


Figure 5.7: Optimal collection system layout for the base case of Test 3.

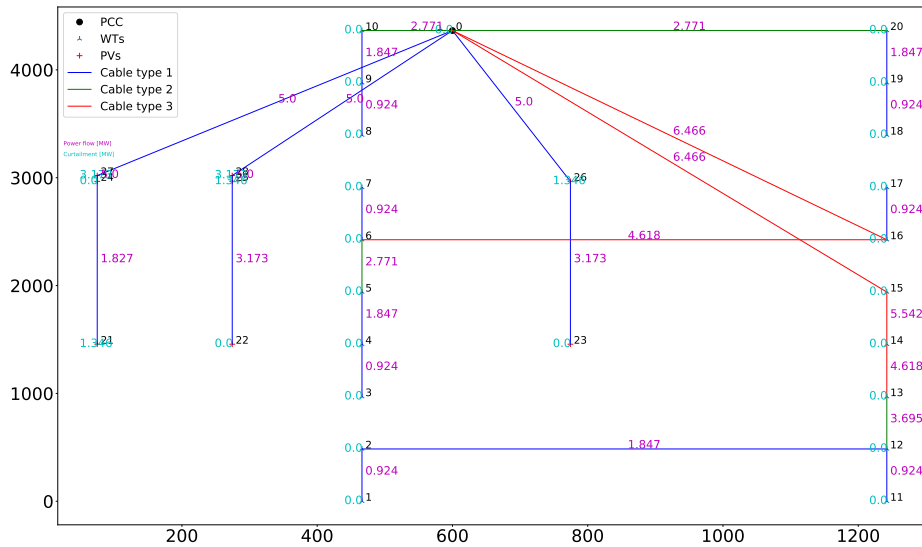


Figure 5.8: Optimal collection system layout for the base case of Test 3 layout when forcing PV systems to be connected in series.

Another advantage that results from building a common electrical infrastructure for the energy technologies wind and solar PV and proves its profitability, is the increased utilisation factor. The installation of cables that collect the power flow from the energy generated in both the WTs and the PV systems allows the cable to be in use during longer hours. Whereas if a cable is only used for solar PV, it will not reach its full capacity (or not even be used at all) during the full range of night-time hours.

For this reason, the utilization factor of the main feeders is calculated for Test 3 and for the Base Case. From Test 3, the strategy that yields the best solution, which is strategy S1, is selected for the calculation. The results obtained show that when running the Base case, the utilization factors of the main feeders, cables connecting the PCC to node 14 and cable connecting the PCC with node 9 (see Figure 5.7), are 26.40% and 22.39%, respectively. On the other hand, the cable selected for the calculation of the utilization factor in Test 3, strategy S1 is cable 0-8. This particular cable is chosen as it connects 8 WTs and 3 PV systems, as it can be seen in Figure 5.6. The value obtained is of 53.40%, which represents an increase of 103% and 138.5%, with reference to the 26.40% and 22.39% values obtained from the Base cases.

Table 5.4 displays a summary of the most relevant results extracted from the conducted analyses.

	Optimal solution	Profitability Increase
Strategy 0	€ 47,104,251.01	
Strategy 1	€ 28,518,115.08	39.46%
Strategy 1	€ 28,518,115.08	
Base Case (independent collection systems)	€ 35,764,540.41	20,26%
	Main feeder utilization factor	Increase
Strategy 1	53.40%	
Base Case (cable with only Wind)	22.40%	138.42%
Strategy 1	53.40%	
Base Case (cable with only PV)	22.78%	134.42%

Table 5.4: Overview of results obtained from the evaluation of Test 6.

Furthermore, it is worth mentioning that for the present test, the computational time elapsed for solving the optimization problem rises substantially as a consequence of its elevated complexity with respect to Tests 1 and 2. The total time incurred by the solver to find the optimal solution of Test 3 through branch and cut optimization is of 3612.19 seconds, whereas for Tests 1 and 2 is of 22.95 and 19.41 seconds, respectively.

All things considered, the results obtained from Test 3 are much more conclusive. It can be appreciated how beneficial it is to design a shared electrical infrastructure for wind and solar PV, in which the cables are dimensioned considering power values resembling the real generation values. Hence, taking into account the negative correlation of wind and solar.

Moreover, throughout the project, it has been mentioned on numerous occasions how beneficial is the integration of wind and solar in the same plant, with shared electrical infrastructure. For this purpose, the result of Test 3 obtained for strategy S1, is chosen to be assessed. More specifically, the behavior of the power flow through the cable linking nodes 0 and 8. The plots in Figure 5.9 intend to illustrate this fact. The first subplot is a representation of the wind power series of the 8 WTs that are connected to cable 0-8, over the course of a week. Likewise, the solar series of 3 PV systems connected to the same cable are plotted in the second subplot. Finally, the third graph depicts the actual power that flows through the aforementioned cable, obtained from the optimization problem.

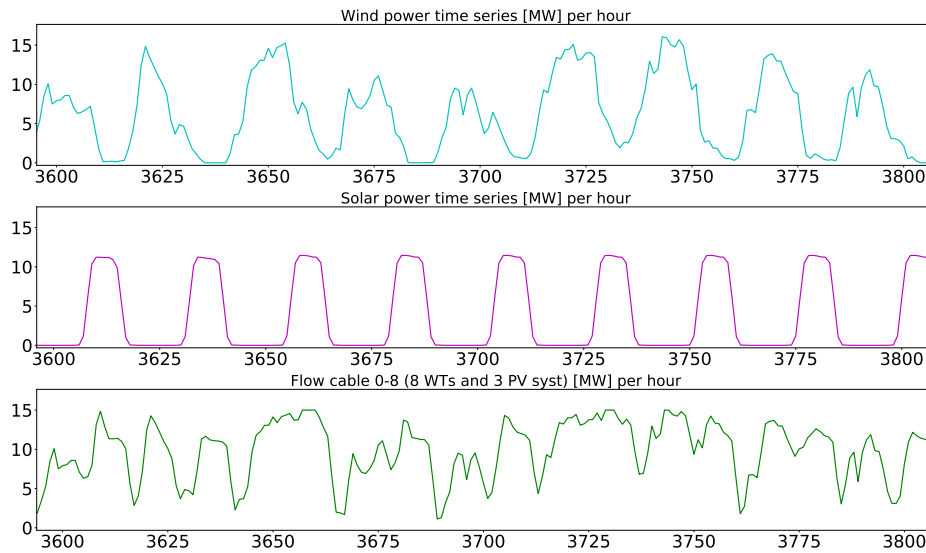


Figure 5.9: Top: Time-series of power generated by 8 WTs over 1 week. Middle: Time-series of power generated by 3 PV systems over 1 week. Bottom: Power flow through cable 0-8 connecting 8 WTs and 3 PV systems over 1 week (3600 hour to 3800 hours).

It can be appreciated how the negative correlation between both generation technologies allows the power flow through the cable to be significantly more constant and to slightly reduce the inherent fluctuations from the operation of both technologies independently. The power supply becomes more dispatchable and moments of very low or even zero production can be more easily avoided. On the other hand, the fact that only a few cases arise in which the generation from the RES exceeds the capacity of the installed cable (15 MW) is representative of a well performed dimensioning. If only PV systems were connected to this cable, generation would only be available during daylight hours and it would be impossible to meet the demand. Besides, if more PV systems were connected to the cable in question, the positive effect of the combination would become even greater. Due to the fact that during periods of low wind generation, the energy production of solar would increase and it would result in a flatter combined power flow.

Finally, a sensitivity analysis is conducted to test the robustness of the outcomes and evaluate the sensitivity of the conclusions and results to variations of inputs entered in the optimizer. Due to the significant weight the electricity price has

on the objective function, it is decided to assess how variations in this parameter can affect the optimal solution proposed by the model.

The price of electricity introduced in Test 6 is increased from an initial value of 82€/MWh to 100€/MWh, to evaluate its influence on the solution. Analogously, the same variation is implemented in the Base Case in order to compare both results. Figures 5.10 and 5.11 illustrate the layouts resulting from the consideration of the aforementioned electricity price. The values of the optimal solutions obtained from both cases are 28,429,440.81€ and 36,852,570.71€, respectively. This proves that for a scenario with higher electricity prices, the implementation of a shared electrical infrastructure is still more advantageous than the installation of independent collection systems.

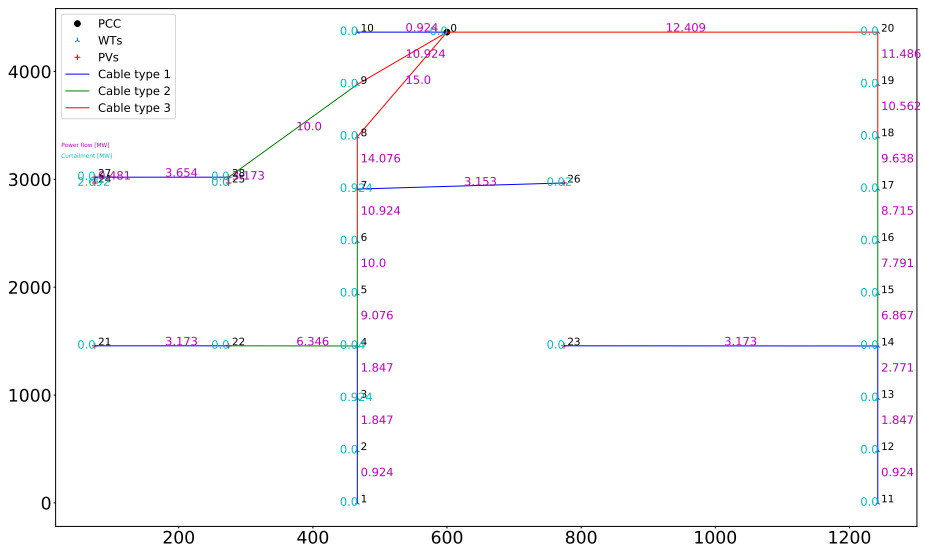


Figure 5.10: Optimal collection system layout when applying strategy 1 to Test 3 with an electricity price of 100€/MWh.

CHAPTER 6

Conclusions and Future work

6.1 Conclusions

The aim of this project is to investigate the economic profitability of designing a shared collection network for a Hybrid Power Plant (HPP) composed of two Renewable Energy Sources (RES), namely wind and solar photovoltaic (PV). To do so, a mathematical optimisation model has been built to find the optimal electrical infrastructure, minimizing investment costs as well as curtailed energy throughout the plant's lifetime. This topic is of crucial interest due to the geographical closeness of the generation assets and their complementary nature.

For this purpose, three different configurations, referred to as tests throughout the thesis, have been proposed and analysed. The latter consist of the combination of diverse HPP layouts and system specifications, namely cables and grid rated capacities. Each test has been evaluated under different clustering strategies, defined to reduce the computational time and complexity of the optimisation model.

After conducting the analysis of all the tests, Test 3, in which the renewable generation technologies present similar installed powers and a grid rated capacity of ca. 50% of the total installed capacity, is found to be the most realistic one, thus leading to the most reliable results. Then, the optimal solution from the strategy leading to the lowest cost (i.e., strategy S1) is identified and compared to the solution obtained when running the Base Case (i.e., nominal power operation and independent collection systems). It is proven that it is substantially more economically profitable to design a shared electrical infrastructure for the RES, leading to a cost of 28.52 M€, instead of designing them independently, resulting in 35.76 M€. Quantitatively, the profitability of the former alternative is improved by 20.25%, with respect to the latter. Additional benefits resulting from installing a shared electrical collection network are, a more efficiently exploited electrical infrastructure and an increased cables utilization factor. The latter shows a value of 22.39% in the Base Case, and of 53.40% for strategy S1, representing an increase of 138.5%. It is also noted that for all the assessed tests, strategy S1 exhibits a better performance. This demonstrates that, in terms of cost-effectiveness, it is undoubtedly more beneficial to use power generation values of wind and solar that reflect their negative correlation, rather than opting

for the conventional procedure of assuming constant nominal power operation.

It is anticipated that this work will serve as a first step for the development of more comprehensive models aiming at designing the collection network of HPPs, and ultimately encourage the implementation of such plants. Indeed, this study contributes to enhance their economic profitability.

6.2 Recommendations for Future work

Several limitations and assumptions are highlighted throughout the thesis, and further recommendations are therefore suggested in the followings, to improve the comprehensiveness and reduce the uncertainties of future studies on HPPs:

- Evaluation of more precise clustering strategies for the power series to assess a potential enhancement of the model.
- Analysis of optimal HPP topology, (i.e., installation of shared or individual transformer) when considering power losses incurred in cables, in order to assess the trade-offs between the cost associated to electrical losses in the cables and cost of the installed transformers.
- Study of the result and possible benefits of implementing a DC-coupled HPP for HVAC or HVDC connection.
- Incorporation of a storage technology in the HPP to further enhance the benefits of the RES.
- Utilization of time-varying electricity prices in the Recourse problem in order to make the model more realistic.
- Consideration of the reactive power of cables, in fact interesting for Wind Turbine controllability, may lead to the need of cables having bigger cross-sectional areas.
- Inclusion of the costs of transformers and inverters in the model to assess the system more accurately.

Considering these aspects could broaden the definition of the optimal collection system of an HPP and strengthen the outcomes of the study.

Bibliography

- [1] *Energy transition Outlook 2020*. DNV GL, 2020.
- [2] United Nations. *Sustainable Development Goals (SDGs)*. https://www.undp.org/sustainable-development-goals?utm_source=EN&utm_medium=GSR&utm_content=US_UNDP_PaidSearch_Brand_English&utm_campaign=CENTRAL&c_src=CENTRAL&c_src2=GSR&gclid=CjwKCAjwlrqHBhByEiwAnLmYUB96KycYH-ceo9XYTPWBfn4n3BoC8coQAvD_BwE.
- [3] United Nations. *Paris Agreement*. https://ec.europa.eu/clima/policies/international/negotiations/paris_en.
- [4] International Energy Agency. *World Energy Investment 2020*. IEA, 2020.
- [5] Katherine Dykes, Jennifer King, Nicholas Diorio. “Research Opportunities in the Physical Design Optimization of Hybrid Power Plants.” In: *4th International Hybrid Power Systems Workshop* (2019).
- [6] Windlab. *Construction to start on \$160 million Kennedy Energy Park in North Queensland*. windlab. Dec. 2017.
- [7] Kaan Deveci, Burak Barutçu, Emre Alpman, Akın Taşçıkaraoğlu. “Electrical Layout Optimization of Onshore Wind Farms Based on a Two-Stage Approach.” In: *IEEE Transactions on Sustainable Energy* (2020).
- [8] Alessandra Cossu. “Optimal sizing of hybrid power plant.” In: (July 2020).
- [9] Arnau González, Jordi-Roger Riba, Antoni Rius, Rita Puig Escola. “Optimal sizing of a hybrid grid-connected photovoltaic and wind power system.” In: *Journal Applied Energy* (2015).
- [10] Pragya Nema, R.K. Nema, Saroj Rangnekar. “A current and future state of art development of hybrid energy system using wind and PV-solar: A review.” In: *Renewable and Sustainable Energy Reviews* (2009).
- [11] *Renewable Hybrid Power Plants: Exploring the benefits and market opportunities*. Wind Europe, July 2019.
- [12] Petersen, Lennart; Hesselbæk, Bo; Martinez, Antonio; Borsotti-Andruszkiewicz, Roberto M.; Tarnowski, German Claudio; Steggel, Nathan; Osmond, Dave. “Vestas Power Plant Solutions Integrating Wind, Solar PV and Energy Storage.” In: *Proceedings of the 3rd International Hybrid Power Systems Workshop* (2018).

- [13] Badwawi, Rashid Al Abusara, Mohammad Mallick. “A Review of Hybrid Solar PV and Wind Energy System.” In: *Journal Smart Science* (2015).
- [14] Ana Cabrera-Tobar, Eduard Bullich-Massagué, Mònica Aragüés-Peñalba, Oriol Gomis-Bellmunt. “Topologies for large scale photovoltaic power plants.” In: *Renewable and Sustainable Energy Reviews* (June 2016).
- [15] Martina Fischetti, David Pisinger. “Optimizing wind farm cable routing considering power losses.” In: *European Journal of Operational Research* (2018).
- [16] Juan-Andrés Pérez-Rúa, Nicolaos A. Cutululis. “Electrical Cable Optimization in Offshore Wind Farms - A review.” In: *IEEE Access* (2019).
- [17] S. Dutta and T. J. Overbye. “A clustering based wind farm collector system cable layout design.” In: *2011 IEEE Power and Energy Conference at Illinois* (2011).
- [18] Francisco M. Gonzalez-Longatt et al. “Optimal Electric Network Design for a Large Offshore Wind Farm Based on a Modified Genetic Algorithm Approach.” In: *IEEE Systems Journal* 6.1 (2012), pp. 164–172.
- [19] T. D. Daly A. M. J. Pemberton and N. Ertugrul. “On-Shore Wind Farm Cable Network Optimisation Utilising a Multiobjective Genetic Algorithm.” In: *Journal of the Operational Research Society* 37.6 (2013), pp. 659–673.
- [20] Jens Lysgaard. Joanna Bauer. “The offshore wind farm array cable layout problem: a planar open vehicle routing problem.” In: *Journal of the Operational Research Society* 66.3 (2015), pp. 360–368.
- [21] Alain Hertz et al. “Optimizing the design of a wind farm collection network.” eng. In: *Infor* 50.2 (2012), pp. 95–104. issn: 19160615, 03155986. DOI: 10.3138/infor.50.2.095.
- [22] Adelaide Cerveira et al. “Optimal Cable Design of Wind Farms: The Infrastructure and Losses Cost Minimization Case.” In: *IEEE Transactions on Power Systems* 31.6 (2012), pp. 4319–4329.
- [23] Juan-Andrés Pérez-Rúa. “Electrical Network Design for Offshore Wind: Analysis, Mathematical Modelling, and Optimization.” In: (May 2020).
- [24] International Finance Corporation. “Utility-Scale Solar Photovoltaic Power Plants.” In: *Renewable and Sustainable Energy Reviews* (2015).
- [25] United States Agency for International Development (USAID). “NTPC Solar Wind Hybrid at Kudgi. White paper on Design Approach for Wind-solar Hybrids.” In: (2017).

-
- [26] Kaushik Das et al. “Enhanced Features of Wind based Hybrid Power Plants.” In: *Proceedings of the 4th International Hybrid Power Systems Workshop*. 4th International Hybrid Power Systems Workshop ; Conference date: 22-05-2019 Through 23-05-2019. 2019. URL: <http://hybridpowersystems.org/>.
- [27] Juanita Ojeda. “Hybrid Renewables: collaborating towards a greener future.” In: General Electric Company, 2019.
- [28] Junxian Li, Weihao Hu, Xiawei Wu, Qi Huang, Zhou Liu, Cong Chen, Zhe Chen. “Cable Connection Optimization for Onshore Wind Farms Considering Restricted Area and Topography.” In: *IEEE Systems Journal* (2020).
- [29] International Energy Agency. *Electricity Market Report: December 2020*. IEA, 2020.
- [30] David Feldman, Mark Bolinger, Paul Schwabe. “Current and Future Costs of Renewable Energy Project Finance Across Technologies.” In: *NREL/TP-6A20-76881* (2020).
- [31] IBM. *Introducing IBM ILOG CPLEX Optimization Studio 20.1.0*. <https://www.ibm.com/docs/en/icos/20.1.0?topic=2010-introducing-ilog-cplex-optimization-studio>.

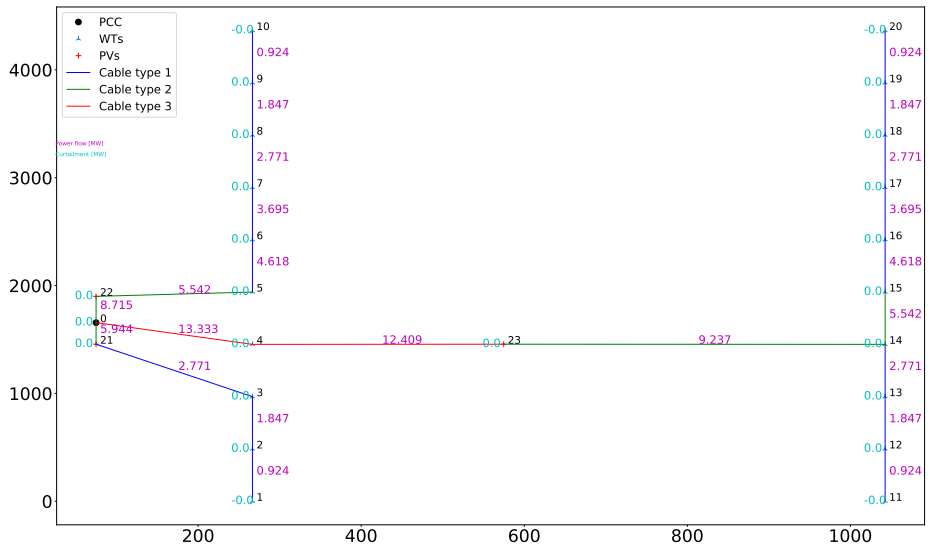


Figure 2: Optimal collection system layout when applying strategy 1 to Test 2.

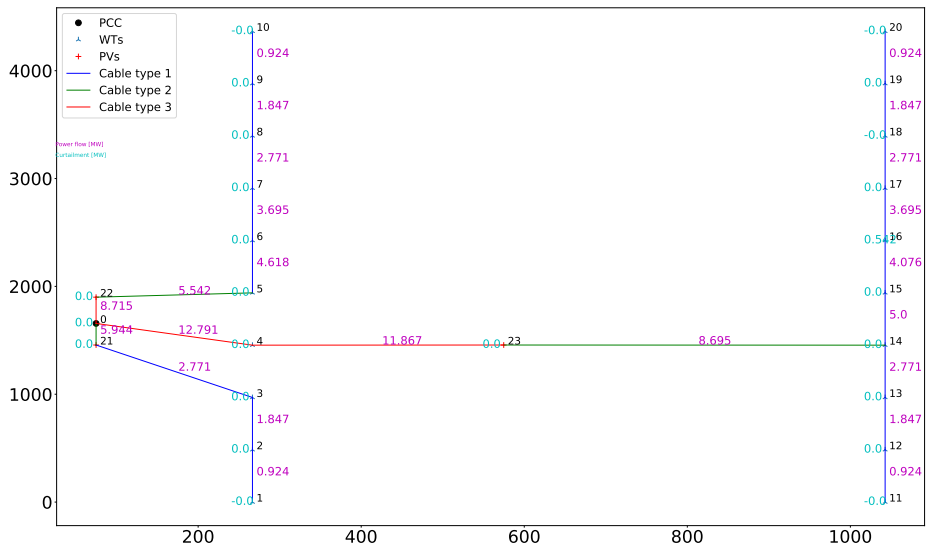


Figure 3: Optimal collection system layout when applying strategy 2 to Test 2.

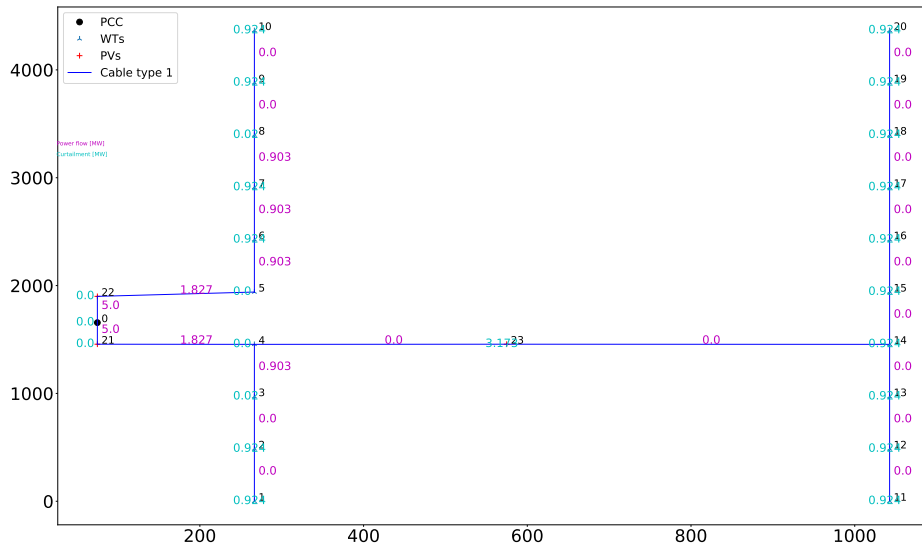


Figure 4: Optimal collection system layout when applying strategy 3 to Test 2.

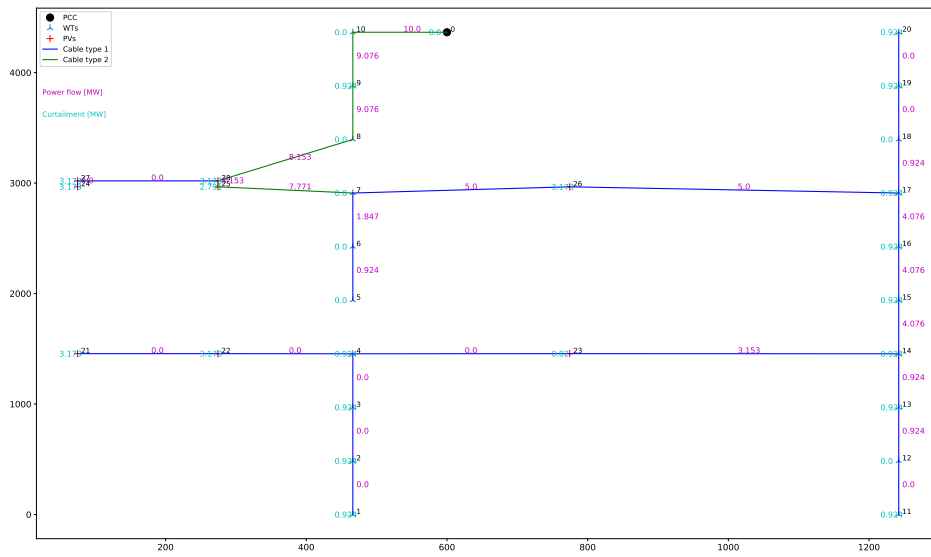


Figure 6: Optimal collection system layout when applying strategy 3 to Test 3.